Paper:
Song, X., Zhang, J., AghaKouchak, A., Roy, S., Xuan, Y., Wang, G., He, R., Wang, X. & Liu, C. (2014). Rapid urbanization and changes in spatiotemporal characteristics of precipitation in Beijing metropolitan area. *Journal of Geophysical Research: Atmospheres, 119*(19), 11,250-11,271.

http://dx.doi.org/10.1002/2014JD022084

Rapid urbanization and changes in spatio-temporal characteristics of precipitation in Beijing metropolitan area

Xiaomeng Song[1,2], Jianyun Zhang[1,2], Amir AghaKouchak[3], Shouraseni Sen Roy[4],Yunqing Xuan[5], Guoqing Wang[1,2], Ruimin He[1,2], Xiaojun Wang[1,2], and Cuishan Liu[1,2]

[1]State Key Laboratory of Hydrology-Water Resources and Hydraulic Engineering, Nanjing Hydraulic Research Institute, Nanjing, Jiangsu, China

[2]Research Center for Climate Change, Ministry of Water Resources, Nanjing, Jiangsu, China

[3]Center for Hydrometeorology and Remote Sensing, University of California, Irvine, Irvine, California, USA

[4]Department of Geography and Regional Studies, University of Miami, Coral Gables, Florida, USA

[5]College of Engineering, Swansea University, Swansea, Wales, UK

Corresponding author: X. Song, Department of Hydrology and Water Resources, Nanjing Hydraulic Research Institute, Guangzhou Road 225, Gulou District, Nanjing 210029, China (xmsong.cn@gmail.com, xmsong@nhri.cn)

Key Points

- Assessed changes in precipitation patterns in Beijing under rapid urbanization
- A significantly decreasing trend in annual precipitation is observed
- A significant increasing trend in extreme precipitation intensity is observed

Abstract:

This study investigates changes in temporal trends and spatial patterns of precipitation in Beijing over the last six decades. These changes are discussed in the context of rapid urbanization and the growing imbalance between water supply and demand in Beijing. We observed significant decreases in precipitation amounts from 1950 to 2012, with the annual precipitation decreasing by 32% at a decadal rate of 28.5 mm. In particular, precipitation decrease is more pronounced in the summer and warm seasons when water use is at its seasonal peak. We further analyzed hourly precipitation data from 43 rain gauges between 1980 and 2012 to examine the spatio-temporal characteristics of both precipitation amount and intensity across six distinct sub-regions in Beijing. No significant spatial variations in precipitation changes were identified, but slightly greater amounts of precipitation were noted in the urban areas (plains) than in the surrounding suburbs (mountains), due to the effect of urbanization and topography. Precipitation intensity has increased substantially, especially at the hourly duration, as evidenced by the more frequent occurrence of extreme storms. The observed decreased water availability and the increase in extreme weather events require more integrated water management, particularly given the expectation of a warmer and more variable climate, the continued rapid growth of the Beijing metropolis, and the intensifying conflict between water supply and demand.

Key words: precipitation pattern, spatio-temporal variation, trend, precipitation intensity, Beijing

Index Terms

1854 Precipitation

1803 Anthropogenic effects

1616 Climate variability

1632 Land cover change

1. Introduction

Today, more than half of the world's population resides in urban areas, a total projected to reach almost 70% by 2050 [*Li et al.*, 2013; *Seto et al.*, 2011; *United Nations*, 2012]. Along with the rapid population growth, urban expansion also entails artificial changes in land use/cover and decreased albedo [*Han et al.*, 2014a]. These population concentrations are marked by built-up landscapes that transform portions of the Earth's natural surface into impervious surfaces that are rougher in texture and far more heterogeneous than those in surrounding rural areas. Such changes have serious ecological and environmental consequences [*Grimm et al.*, 2008], including deforestation and land fragmentation [*Miller*, 2012], local and regional climate change [*Kaufmann et al.*, 2007], alterations of the hydrological cycle [*Jackson*, 2011; *Ladson et al.*, 2006; *Yang et al.*, 2011], and urban heat islands [*Oke*, 1973], etc. The hydrological impacts of urbanization and heat island formation have been of particular concern [*Chu et al.*, 2013; *Du et al.*, 2012; *Fletcher et al.*, 2013; *Ganeshan et al.*, 2013; *Jackson*, 2011]. Specifically, global and regional precipitation changes have been observed for the past few decades across many regions [*Dai*, 2013; *Damberg and AghaKouchak*, 2014; *Hao et al.*, 2013; *Yang and Lau*, 2004], especially in urban areas [*Creamean et al.*, 2013; *Pathirana et al.*, 2014]. Many studies (e.g., the Metropolitan Meteorological Experiment (METROMEX) [*Han et al.*, 2014a], the UK Climate Impacts Programme (UKCIP) [*Russell and Hughes*, 2012], and the HYDROMET Integrated Radar Experiment (HIRE'98) [*Berne et al.*, 2004]) have examined the effect of urbanization on precipitation, and the consensus view is that the key factors are the urban-rural land-surface discontinuity and the concentration of urban aerosols [*Han and Baik*, 2008; *Li et al.*, 2011; *Pinto et al.*, 2013; *Wang et al.*, 2012a; *Yang et al.*, 2014].

As one of the world's largest metropolises, Beijing has experienced accelerated urban expansion over the past four decades. The built-up area has increased from 184 km^2 to 1,350 km^2 between 1973-2012, with the metropolitan population approaching more than 20 million [*Wu*, 2012; *Yang et al.*, 2014]. Rapid urbanization introduced myriad new challenges, most notably air quality issues, water scarcity crises, and urban flooding problems. Severe rainstorms and flood events in Beijing have become more frequent in recent years. For instance, the storm event of July 21, 2012 produced a rainfall total in excess of 460 mm in 18 hours, resulting in multiple disasters and 79 casualties [*Zhang et al.*, 2013a]. Rapid urbanization also causes the imbalance between water supply and demand to become even more serious. One alarming sign is that aridity and water shortages have become increasingly critical. Recorded observations reveal steadily decreasing precipitation [*Xu et al.*, 2006b; *Zhai et al.*, 2014; *Zhu et al.*, 2012], especially around the Miyun reservoir area, a primary source for Beijing's water supply [*Zhang et al.*, 2009]. In addition, the local effects of declines in precipitation and changes in precipitation pattern – as well as the reasons behind them – have also been of concern in recent years [*Han et al.*, 2014b; *Miao et al.*, 2009; *Sun and Yang*, 2008; *Wang et al.*, 2009; *Zhang et al.*, 2005; *Zhang et al.*, 2009]. To some extent, these studies reveal that the local impact factors play an important role in changes in the spatial characteristics and temporal trends of precipitation.

There are a large number of studies on Beijing's spatial and temporal variations in precipitation [*Xu et al.*, 2006b; *Zhai et al.*, 2014; *Zhang et al.*, 2009; *Zhang et al.*, 2014; *Zhu et al.*, 2012], changes in precipitation patterns [*Li et al.*, 2008; *Wang et al.*, 2012b; *Yin et al.*, 2011], and the urban effects [*Miao et al.*, 2011; *Yang et al.*, 2014; *Zhang et al.*, 2009]. *Li et al.* [2008] and *Wang et al.* [2012b] showed that both rainfall amount and rainfall frequency present high values from late afternoon to early morning and reach the minima around noon. *Zhang et al.* [2009] investigated the influences of urban expansion on summer heavy precipitation using observations and a mesoscale weather/land-surface/urban-coupled model, and showed that the urban expansion can alter the water vapour conditions and lead to a reduction in precipitation. *Miao et al*. [2011] analyzed the impacts of urbanization on summer precipitation using the Weather Research and Forecasting (WRF) model, and concluded changes in precipitation depends on the degree of urbanization. Most previous studies, however, are limited by the fact that they rely on the data obtained from only a few scattered weather stations focused at the smaller-scale level of meteorological subdivisions and do not address water resource problems caused by changes in precipitation. Even fewer of previous studies have recognized the important role played by topography and urban expansion in the distribution of precipitation, as they can only be well analyzed through the use of more detailed regional subunits and a significantly greater number of rain gauges. This study aims to remedy these shortcomings, and its objectives are to (1) analyze the temporal variations in annual and seasonal precipitation from 1950-2012, highlighting the changes in the spatio-temporal characteristics of warm-season (June-September) precipitation across six sub-regions from 1980-2012 within the Beijing area, (2) examine the influence of local factors, especially urbanization and topography on the changes in precipitation, and (3) discuss the water related issues linking the changes in precipitation patterns in Beijing.

This paper is organized as follows. The study region, the data and methods are described in Section 2. In Section 3, the temporal variability and spatial distribution of precipitation are discussed, including annual and seasonal precipitation amount, and warm seasonal precipitation intensity. Section 4 explores the possible causes of the observed changes in precipitation patterns. Section 5 focuses on implications for water crises in Beijing. Section 6 summarizes the conclusions and remarks.

2. Data and methods

2.1 Study area and data sources

The Beijing metropolitan area comprises a total area of approximately 16,410 km^2, of which roughly 38% is relatively flat and 62% is mountainous (Figure 1). The latter is located primarily to the north and west, with elevations averaging 1,000-1,500 m, while the lowland zone lines in the center and southeast, with elevations ranging from 20 to 60 m. Beijing has a monsoon-driven humid continental climate, characterized by hot humid summers and cold dry winters. The mean annual temperature is 11-12℃, and the mean annual precipitation is approximately 600 mm [*Zhai et al.*, 2014].

In order to effectively analyze the spatial variability of rainfall, the selected stations cover all 16 districts in the Beijing metropolitan area, including 14 urban and suburban districts (Dongcheng, Xicheng, Chaoyang, Haidian, Fengtai, Shijingshan, Tongzhou, Shunyi, Changping, Daxing, Mentougou, Fangshan, Pinggu, and Huairou) and two rural counties (Miyun and Yanqing), as shown in Figure 1. To emphasize the important role of terrain in the local distribution of precipitation, *Wang et al.* [2012b] suggested to divide Beijing into four zones: urban, suburban, northern mountainous, and southern mountainous areas. Allowing for Beijing's ongoing urban expansion, we follow a similar approach that uses a more detailed matrix of six subregions: the urban area (UA), the inner suburb area in the south (ISAS), the inner suburb area in the north (ISAN), the outer suburb area (OSA), the southwest mountainous area (SWMA), and the northwest mountainous area (NWMA) (see Figure 1). Despite the comparatively large number of rain gauges deployed, only a limited number have long-term records. As such, the information from only those stations that provide precipitation data for at least three decades is collected and analyzed. As a result, the 43 stations meeting these criteria are mapped in Figure 1 and listed in Table 1.

[Figure 1 and Table 1 should be inserted here]

Monthly and annual mean precipitation data in the Beijing metropolitan area, calculated and provided by the Beijing Hydrological Center of the Beijing Water Authority and based on a network of 16 rain gauges across Beijing, as shown in Figure S1, are used to detect the temporal trend of precipitation between 1950 and 2012. Overall, most of Beijing's precipitation occurs during the warm season (June-September). Therefore, the daily and hourly precipitation data in the warm season from 1980-2012 were collected from 43 stations to analyze the spatial and temporal characteristics of precipitation in Beijing. The density of observations is greatest in the central urban and the surrounding areas, while the coverage of stations in the mountainous zone is relatively sparse. Although some stations were installed as far back as the late 1950s, the observation networks and comprehensive record-keeping did not commence until the 1980s.

Annual mean temperature data at Beijing Guanxiangtai weather station (Figure 1) are obtained from the China Meteorological Data Sharing Service System (http://cdc.cma.gov.cn/home.do), which is overseen by the Climatic Data Center, National Meteorological Information Center, China Meteorological Administration. Data on urban built-up areas in Beijing are obtained from the Beijing Statistical Annals and China Statistical Yearbook, which is released by the Beijing Statistical Bureau and the State Statistics Bureau and published yearly by China Statistical Press. All water resources data involving the water use and demand data are obtained from the Beijing Water Resources Bulletin and the Beijing Hydrological Regime Annual Report, which is released by the Beijing Water Authority.

2.2 Methods

Four techniques were selected to identify and explain spatio-temporal variations of precipitation in Beijing. First, linear regression and the Mann-Kendall (M-K) test were used to assess the precipitation trends. Second, the spatial distributions of these trends were analyzed by the M-K test and spatial interpolation. Then, the temporal variations were investigated using a moving-average method to cross-check results revealed by the M-K test and linear regression.

2.2.1 Linear regression

Linear regression is a parametric method used to obtain the slope (or trend) of hydro-meteorological variables over time [*Mosmann et al.*, 2004]. The linear regression equation can be represented as:

$$y = a + bx + \varepsilon \tag{1}$$

The slope b can be used as an indicator of trend and is calculated as:

$$b = \frac{n\sum_{i=1}^{n} x_i y_i - \sum_{i=1}^{n} x_i \sum_{i=1}^{n} y_i}{n\sum_{i=1}^{n} x_i^2 - \left(\sum_{i=1}^{n} x_i\right)^2} \quad (2)$$

where y_i is a climatic factor, x_i is time, and n is the length of the time sequence. A statistically significant b indicates the slope of a linear trend.

2.2.2 M-K test

The M-K test [*Mann*, 1945; *Kendall*, 1975] is recommended by the World Meteorological Organization (WMO) as a non-parametric method for trend detection because of its robustness and simplicity. The M-K test has been widely used to assess the significance of monotonic trends of hydro-meteorological variables [*Zhang et al.*, 2011, 2012]. For a given time series $X = (x_1, x_2, \ldots, x_n)$, the M-K test statistic S is defined by:

$$S = \sum_{i=1}^{n-1} \sum_{j=i+1}^{n} \mathrm{sgn}(x_j - x_i) \quad (3)$$

where n is the data record length, x_i and x_j are the sequential data values, and the function sgn(x) is defined as:

$$\mathrm{sgn}(x) = \begin{cases} 1 & x > 0 \\ 0 & x = 0 \\ -1 & x < 0 \end{cases} \quad (4)$$

The statistic S is approximately normally distributed with the mean $E(S) = 0$ and variance as

$$Var(S) = \frac{n(n-1)(2n+5) - \sum_{i=1}^{n} t_i(i)(i-1)(2i+5)}{18} \quad (5)$$

where t_i is considered as the number of ties up to sample i. The standardised normal test statistic Z is given by

$$Z = \begin{cases} \frac{S-1}{\sqrt{Var(S)}} & S > 0 \\ 0 & S = 0 \\ \frac{S+1}{\sqrt{Var(S)}} & S < 0 \end{cases} \tag{6}$$

The null hypothesis H_0 that there is no trend in the records, is rejected (not rejected) if the statistic Z is greater (less) than the critical value of $Z_{\alpha/2}$ obtained at the level of significance α. A positive (negative) value of Z signifies an upward (downward) trend [*Bao et al.*, 2012].

Furthermore, the nonparametric Mann-Kendall's test can also be used to detect the change points of time series [*Partal and Kahya*, 2006]. This test sets up two series, a forward one (*UF*) and a backward one (*UB*). The *UF* is similar to the Z values that are calculated for the data. Following *Partal and Kahva* [2006], the steps are:

a) The magnitudes of x_i (i = 1, 2, …, n) mean time series are compared with x_j (j = 1,2,…, i-1). For each comparison, the number of cases $x_j > x_i$ is counted and denoted by r_i.

b) The test statistic S_k is

$$S_k = \sum_{i=1}^{k} r_i \quad (k=2,3,\ldots,n) \tag{7}$$

c) The mean and variance of the test statistic are calculated as

$$E(S_i) = \frac{i(i-1)}{4} \tag{8}$$

$$Var(S_i) = \frac{i(i-1)(2i+5)}{72} \tag{9}$$

d) The sequential values of the statistic *UF* are computed as

$$UF_i = \frac{S_i - E(S_i)}{\sqrt{Var(S_i)}} \quad (i=1,\ 2,\ \ldots,\ n) \tag{10}$$

Similarly, the values of *UB* are computed backward from the end of the time series. If the *UF* and *UB* curves intersect and then diverge and acquire specific threshold values, then a statistically significant trend exists [*Tabari et al.*, 2011]. The point of intersection shows the approximate change point at which the trend begins [*Mosmann et al.*, 2004].

2.2.3 Moving-average method

The simple moving-average method is typically used to test the trend in a long-time series [*Zhai et al.,* 2014]. A moving-average method is used to smooth out short-term data fluctuations and highlight longer-term trends. The moving-average method can be expressed as:

$$F(t) = \frac{(x(t) + x(t-1) + ... + x(t-(N-1))}{N} \tag{11}$$

in which $x(t)$ is the actual value at time t of the original time series, N is the average periodicity, and $F(t)$ indicates the predicted values of the t stage. The threshold between short-term and long-term depends on the application, and the parameters of the simple moving-average method are set accordingly. A commonly used five-year average is used in this study.

2.2.4 Spatial interpolation

Spatial interpolation as a necessary tool has been widely used in building precipitation distribution from rain-gauge data. There are many methods available, such as Polynomial, Nearest-neighbour, Inverse Distance Weighted (IDW), Kriging and its variants. The normal Kriging method is selected for this study because it contains the highest correlation coefficient calculated from the cross-validation test [*Garen and Marks*, 2005; *Liang et al.*, 2011a]. Moreover, this technique also produced the closest representation of the real values, which was in the form of the lowest difference between the observed and predicted values of known data points [*Roy*, 2009]. Thus, Kriging is implemented on all 43 rain gauges to obtain the spatial pattern of precipitation in the study area.

3. Results

3.1 Temporal variability and trends of precipitation amounts in the Beijing area

The mean annual precipitation from 1950-2012 varies from a low of 383.9 mm in 1965 to a high of 1,005.6 mm in 1954, with a mean of 584.7 mm. A decrease in mean annual precipitation is observed for Beijing after 1960. Although the mean annual precipitation exhibits large inter-annual variability, it has decreased overall by almost 32% during this period at a rate of 28.5mm/10a (Figure 2). Five-year moving average curves emphasize the trends and variability in the annual precipitation series. The decadal variability of precipitation indicates that alterations of wet and dry periods occur over time. For example, 1954-1964 is a wet period followed by a gradual decrease of annual precipitation to its long-term average value from 1965-1975. Another short wet period occurred from 1976-1979, exhibiting a narrow magnitude. Beijing experienced a relatively longer dry period in the 1980s and early 1990s, with 1980 being the third driest year during the 1950-2012 time period. A transitory wet period in the mid-1990s occurred next, followed by another long and more severe dry spell from 1997-2011, during which 1999 was the second driest year on record since 1950. As for the maxima, Figure 2 also shows that the precipitation in 2012 exceeded 700 mm, the highest value in the last 18 years and the second largest over the past three decades. The declining annual precipitation trend in Beijing is consistent with the trends in the Haihe River basin [*Bao et al.*, 2012; *Chu et al.*, 2010] as well as northern China in a larger context [*Cong et al.*, 2010] over the past 60 years. For seasonal precipitation, the warm-season (June-September) precipitation accounts for about 83.5% (60.13%-91.53%) of the annual precipitation from 1950-2012. The decreasing trend (29.7

mm/decade) of warm-season precipitation is consistent with that of annual precipitation (both statistically significant at 0.05 significance level). At the seasonal level, precipitation in spring and autumn shows a slowly increasing (statistically insignificant) trend of 0.7 mm/decade and 0.9 mm/decade, respectively, while the summer precipitation declined by 32.8 mm/decade (statistically significant). In comparison, the trend of mean precipitation in winter shows little change, fluctuating within a narrow range. Thus, we attribute to the fact that the steadily increasing trend in the spring and autumn is unable to offset the remarkable decrease in the summer, which plays a dominant role in the trends of overall annual precipitation.

A similar conclusion can also be drawn from Figure 3, which shows decadal changes in precipitation according to seasons. Significant inter-decadal and inter-annual variations in precipitation amounts are revealed. Mean and median values of summer, warm-season, and annual precipitation from 2000-2012 are all lower than those of earlier decades. We also observe larger inter-annual variations in the 1950s compared with other decades. In contrast, the mean and median values in spring and autumn first decline from the 1950s and then rise in the 1980s. Additionally, there is no stable variation pattern in winter, with a state of disorder.

[Figure 2 and Figure 3 should be inserted here]

The trends obtained by the M-K method are shown by the red (*UF*) and blue (*UB*) solid lines, respectively, in Figure 4, and the horizontal dashed lines correspond to the confidence limits at the significance level of $\alpha = 0.05$. A statistically significant trend of increasing or decreasing precipitation is indicated if the red solid line crosses over the dashed line. There is no significant trend for the autumn and winter (Figures 4c-4d), but a short-term significant decrease occurs for the spring during the 1958-1963 and 1972-1979 periods (Figure 4a). Summer and warm-season precipitation exhibit a declining trend for most years, particularly during the 1999-2012 period (Figures 4b and 4e). The analogous trend occurs for annual precipitation, with the significant decrease commencing in 2001 (Figure 4f).

Monthly precipitation amounts and their percentage shares of annual precipitation are displayed in Figure 5. Results indicate that monthly precipitation patterns do not change significantly. It is clear that a large proportion of annual precipitation amount occurs in the warm season (76.4-82.6%), especially during July (27.5-36.8%) and August (21-31.8%). The maximum contributing months to the annual precipitation amount vary for different decades. In the 1950s and 1980s, the August contribution is larger than that from July, while in the other decades, the August contribution is less than that from July. As discussed earlier, we also find that the contribution from both July and August to the total precipitation shows a remarkable decreasing trend since the 1980s, while that of June and September shows a slight increasing trend. Figure 5b clearly shows that the precipitation amount in July (August) during 1980-2012 has a remarkable decreasing trend, ranging from 209.5 (191.3) mm down to 167.3 (131.1) mm. Thus, the decreases in monthly contributions and precipitation amounts for July and August are a dominant factor in the decreases in summer and warm-season precipitation.

[Figure 4 and Figure 5 should be inserted here]

3.2 Spatial characteristics of warm season precipitation

Precipitation records collected from 43 stations over the period of 1980-2009 are used to analyze the inter-decadal spatial variations in warm season precipitation (Figure 6). The records are further divided into three decades: 1980-1989, 1990-1999, and 2000-2009. In the 1980s (Figure 6a), more precipitation occurs in the northeast mountainous area, with the highest totals of around 600 mm occurring at stations near HSY (591.5 mm) and ZLY (586.6 mm). A relatively high mean precipitation amount (> 500 mm) is recorded for the plains areas of the northeastern part of the OSA. In the SWMA and NWMA regions, the mean precipitation amount is usually less than 400 mm, with the minimum precipitation less than 300 mm recorded at the GT station. We also find an increase in precipitation in the central urban area around the SLZ and YAM stations, with the highest record surpassing 450 mm.

For 1990-1999 (Figure 6b), the highest precipitation amount also occurs in the northeast near the HSY station (≥ 600 mm); a secondary center of precipitation occurs at the Huairou and Miyun reservoirs, with precipitation exceeding 550 mm. Similar to the 1980s, the precipitation amount in the central urban area surpasses that of the suburb area, with the lowest values recorded for stations located primarily in the NWMA and SWMA. However, it was found a small area with high amount in the southwestern sub-region at the ZF station. Overall, there was more precipitation in the 1990s than that of the 1980s, as shown in Figure 6d.

Since 2000 (Figure 6c), the mean maximum precipitation decreases to about 525 mm. On the whole, spatial patterns of precipitation do not change appreciably between 1980 and 2009, indicating only slight variations at the decadal level. Observed results show that precipitation amounts is higher in the eastern part than in the west. Moreover, precipitation in the plains areas is greater than in the mountainous areas, which is also concluded by *Zhai et al.* [2014]. Interestingly, the central urban area does show a relatively greater precipitation amount, which may well be linked to the urbanization effects and land use/cover change (an issue discussed later in Section 4.1).

Figure 6 also examines the decadal precipitation variation in terms of its spatial distribution based on the 43 rain gauges. Overall, precipitation is declining after increasing during most of the past three decades. This trend is similar to the changes in mean annual precipitation for the same period discussed in Section 3.1, with the largest values occurring in the 1990s and the lowest in the 2000s. Compared to the 1980s, the total warm-season precipitation in the 1990s is greater, except for a few areas in the northeast (Figure 6d). In the 2000s, the largest decreases occurred in the northeastern areas, with the largest decrease (≥ 150 mm) occurring at the ZLY and PG stations (Figures 6e-6f). Another major decrease in precipitation took place around the Miyun and Huairou reservoirs, which decreased more than 100 mm since the 1990s (Figure 6e). Because the Miyun reservoir supplies most of Beijing's water, this reduction in precipitation directly intensified the metropolitan water shortage. Another significant decrease of more than 100 mm is observed in the UA, which accounts for 20-30% of the mean warm-season total precipitation.

It is interesting to see the spatial distribution of the temporal trend at each rain-gauge station. The M-K test results for warm-season precipitation amounts are presented in Figure 7. We found that 29 stations experienced a decreasing trend. Amongst these stations, which are located mainly in the mountainous and outer suburb area, three stations (QJD, YQY, and PG) experienced by significantly decreasing precipitation at the 95% confidence level. Fourteen stations exhibit increasing precipitation (not statistically significant), and are mostly found mostly in the urban (6 stations except for the YAM station) and inner suburb areas (7 stations). Figure 7 also reveals that most stations located in the urban area are marked by non-significant increases in precipitation.

[Figure 6 and Figure 7 should be inserted here]

The changes in trends and variation of mean warm-season precipitation for the six sub-regions from 1980-2012 are shown in Figure 8. In all six sub-regions, the precipitation amounts first increase and then decline from 1980-2012. Except for the NWMA, the other five areas have one or two change points. In general, the change points of the four plains areas occur at the end of the 1990s, with the other change points in the ISAN occurring in 2011. The change point of the SWMA occurs at the beginning of the 21st century, and those for the NWMA occur around the same time. The precipitation amounts in the four plains areas exhibit a significant increasing trend towards the end of the 1980s and/or the early 1990s at the level of $\alpha = 0.05$, especially for UA and ISAS (significant at the level of $\alpha=0.01$). Moreover, the decreasing trends in the four plains areas in the 2000s are not statistically significant at either of these two levels.

[Figure 8 should be inserted here]

3.3 Spatio-temporal characteristics of precipitation intensity

The precipitation intensity is another important quantity in our analysis as it is one of the key factors in determining urban drainage design and flood control. In this study, two indices related to precipitation intensity have been calculated and analyzed, namely the hourly precipitation intensity and maximum 1hr precipitation intensity. Hourly precipitation intensity has been widely used by climatologists to analyze variations in precipitation [*Wang et al.*, 2012b; *Yang et al.*, 2013]; maximum 1hr precipitation intensity is mostly used in flood control analysis and forecasting. The definition of hourly precipitation intensity provided by *Oke and Musiake* [1994] is used here. As the term implies, the maximum 1hr precipitation is the maximum amount of precipitation that occurs within a continuous one-hour in a year. To a certain extent, the maximum 1hr precipitation intensity can be regarded as an index to examine the extreme precipitation events.

Overall, the spatial variations of precipitation intensity are similar to the spatial distribution of precipitation amount (Figures 9a-9b). The higher values occur most frequently in the plains area, whereas lower values are confined primarily to the mountainous areas. Figure 9a shows that the greatest hourly mean precipitation intensity appears in the OSA near the MY and ZLY stations; the next-highest values are located in the UA at the SLZ station and in the ISAS at the FS station. In contrast, the lowest values occur in the NWMA near the YQ and QJD stations. As seen in Figure 9a, we can conclude that the spatial pattern of hourly mean precipitation intensity is controlled mainly by topographic factors. To some extent, the effect of urbanization may well be important as we have seen relatively higher hourly mean precipitation intensity appearing in the built-up sections of the metropolis. Similar findings are also obtained from Figure 9b, with the highest total found in the outer suburb area near the MY station and the lowest total in the northwest mountainous area. The reason may lie in the fact that the warm southeasterly and southwesterly winds are forced to rise against the mountains of the west and the north, triggering heightened summer precipitation along the windward slopes and reducing precipitation on the leeward slopes [*Xu et al.*, 2006b]. This can also help to explain the precipitation concentrating in the windward slopes of the mountains surrounding the plains area, such as the ZF, SJD, TYK, HR, MYB, and HSY stations, where the maximum 1hr precipitation is more than 36 mm. Similar to the hourly mean precipitation intensity, high values appear in the UA (SLZ, YAM, GBD and TX) and exceed 36 mm. Hence, the effect of urbanization (e.g., urban heat island, land surface roughness, and aerosol density) on precipitation is also important, and requires further investigation.

Figure 9 also shows the M-K statistical trends of hourly mean precipitation intensity and maximum 1hr precipitation. For hourly mean precipitation intensity, only four among the 43 stations exhibit a significantly increasing trend at the level of α=0.05. They are located mainly in the transition zone between the mountainous and plains areas. We also find that the most stations in the

UA, NWMA and the southern part of the metropolis reveal a rising trend, although not statistically significant, and that most of the stations are found to be downward-trending in the ISAN and OSA. The increasing hourly mean precipitation intensity in the region implies that they are increasingly concentrated in short-duration precipitation events, which concurs with previous studies [*Li et al.*, 2008; *Yang et al.*, 2013]. There are 25 stations with an upward trend in maximum 1hr precipitation (Figure 9d), but two stations (WQ and XYL) display a significant upward trend at the level of $\alpha = 0.05$. The remaining 18 stations show a slight decreasing trend but without statistical significance. We also find that most stations that record higher values in maximum 1hr precipitation, such as the Miyun reservoir, the five stations in the central urban area, and the southern part of Beijing metropolis, exhibit an upward trend.

[Figure 9 should be inserted here]

Another use of the M-K method is to assess trends in precipitation intensity for the six sub-regions (Figures 10 and 11). Figure 10 shows the inter-annual and spatial variation of mean hourly precipitation intensity. The results show a slowly increasing trend in four areas (UA, ISAS, SWMA, and NWMA) and a decreasing trend in the other two areas (ISAN and OSA). Overall, apart from SWMA, the inter-annual variation of the mean hourly precipitation intensity in the other five areas first increases and then decreases. The lowest intensities occur at the end of the 1990s and the beginning of the 2000s. However, the patterns for the UA, ISAS, ISAN, and NWMA shows another increasing trend in the 2000s. Figure 10 also reveals that the mean hourly precipitation intensity in the two mountainous areas has remained at a fairly stable level, while that of the plains areas exhibits more fluctuation. Additionally, Figure 11 also shows the inter-annual variation of maximum 1hr precipitation intensity during the warm season over the past three decades. On the whole, similar to hourly mean precipitation intensity, the maximum 1hr precipitation first rises and then falls. There are major declines in maximum 1hr precipitation in the UA, ISAS, and OSA during the longer-term dry period beginning in 1999. The high amplitudes of this 1hr precipitation for all sub-regions and for all time periods lead to significant changes regarding variance even though there are non-statistically significant changes in mean values for the past three decades. This profile of change is also observed in the inner suburb area (ISAS and ISAN) in the 2000s, together with a surge in maximum 1hr precipitation intensity.

[Figure 10 and Figure 11 should be inserted here]

4 Possible causes of changes in precipitation patterns

It is well known that many factors shape precipitation variation in a region, especially in a large urban area. Local precipitation variation is a response to global and regional water cycles, as well as climate variation, the mechanism of which is highly complicated and beyond the scope of this research. In addition, local factors — such as terrain, urbanization, land use/cover change — produce their own spatial impacts on the precipitation pattern. In this section, we discuss possible causes by first making comparisons to regional precipitation change and then qualitatively analyzing the impacts of topography and urban expansion on precipitation.

4.1 Regional and local climate conditions

Over the past 50 years, precipitation has increased in the northwestern and southern China, but has decreased in northern China [*Cong et al.*, 2010; *Liu et al.*, 2005; *Zhai et al.*, 2005]. Annual precipitation has decreased by about 5% per decade in northern China because onshore monsoon winds have become weaker and water vapor transfer has diminished [*Cong et al.*, 2010; *Xu et al.*, 2006a]. High rise buildings associated with urbanization and temperature differences may also cause wind speed reduction [*Cong et al.*, 2010; *Ren et al.*, 2008]. The decline of precipitation in Beijing is consistent with observations all across in northern China, especially in the Haihe River basin where the city is located. Seasonal precipitation change discussed earlier also comes into play: the significant decrease in summer precipitation and warm-season precipitation, in particular, is a leading contributor to the annual precipitation decline in Beijing (Figures 2 and 3). Although the spring and autumn precipitation exhibit a slightly increasing trend, it cannot offset the decline in summer precipitation and annual precipitation. This is consistent with the work of *Zhai et al.* [2005], which addresses observations for spring and summer, but contradicts their findings for autumn and winter in northern China. According to *Hao et al.* [2007, 2011], the causes of declining summer precipitation in northern China are: (1) the weakening of the Mongolian low, and (2) the decline of water vapor transportion from the southwest wind flow because of the depleting movement of southwest monsoon and southeasterly winds from the western Pacific subtropical high. To some extent, these factors may be the cause of the precipitation decline in the Beijing metropolis. *Wang et al.* [2008] analyzed the temporal and spatial characteristics of precipitation and their statistical relationship to SHWP (Subtropical High over the West Pacific). They found that the impact of the SHWP on precipitation in Beijing displayed a significant interdecadal trend, with most rainstorms steered by the combination of the SHWP and westerly trough. Although the causes of precipitation variation in Beijing are still not fully understood, changes in regional atmospheric circulation obviously play a role and require further investigation. In addition, a worldwide review of global rainfall data has found that the intensity of most extreme precipitation events is increasing across the globe as temperatures rise [*Alexander et al.*, 2006; *Westra et al.*, 2013]. Another avenue of research involves temperature from work by *Zhu et al.* [2012], which knows that the mean temperature in Beijing has increased significantly since the 1950s (Figure 12a).

[Figure 12 should be inserted here]

4.2 Topography impacts

Smith [1979] has comprehensively reviewed the complex subject of orographic rainfall. On the windward side, forced lifting of air masses triggers condensation and precipitation with increasing elevation. Depending on the mountain size and the efficiency of the release processes, precipitation will decrease on the leeward side. Thus, topography strongly influences precipitation patterns by altering both the local wind patterns and the condensation of perceptible water [*Siler and Roe*, 2014; *Smith*, 1979]. Beijing has a typical continental monsoon climate with four distinct seasons. The winter is cold and dry due to northerly winds from high-latitude areas, while the summer is hot and wet because of the east and southeast airflow carrying moisture from the southern Pacific Ocean and the Indian Ocean. Because mountainous areas are located primarily in the northern and western sections of Beijing, precipitation in the low-lying southern and eastern parts of Beijing is greater than that of the western and northern sections. We discovered that the highest precipitation occurs at the interface between the mountainous area and the plains areas, confirming the effect of terrain on precipitation patterns. Data from our rain gauges verify these results, which are corroborated further in the findings we observed for changes in precipitation intensity. However, the specific interactions occurring between the topography and the local climate, which contribute to the unique spatial distribution of precipitation among the various regions, has not been fully understood or examined due to lack of adequate data.

4.3 Urbanization impacts

Urban expansion is known to affect precipitation and previous studies have noted that the amount and frequency of precipitation tends to be greater in urban centers and downwind areas than in the surrounding areas, especially for intense convective precipitation in the summer [*Ganeshan et al.*, 2013; *Zheng and Liu*, 2008]. However, this phenomenon has not been confirmed for Beijing in research by *Wang et al.* [2009] and *Liang et al.* [2011b]. *Xu et al.* [2009] and *Li and Ma* [2011] did observe that the urban effect was apparent for large-scale weak precipitation and local strong precipitation, but it could not be discerned for large-scale intense precipitation events. *Yin et al.* [2011] concluded that Beijing precipitation patterns might be shaped by the combined influences of mountain-valley topography and urbanization. *Wang et al.* [2012a] found that the magnitude of precipitation increases slightly in the Beijing-Tianjin urban areas, and argued that urbanization has the greatest impact on summertime precipitation. In our study, we found that the precipitation within the metropolis is greater than the total in surrounding areas during the 1980s and 1990s, whereas warm-season precipitation in the central urban area decreased by about 100 mm from the 1990s to 2000s and by 60-80 mm from the 1980s to the 2000s (see Figure 7). As shown in Figure 12b, urban development in Beijing increased at an annual increment of 8.453 km^2 from 1980-2000, while the increased in rate is more substantial after 2000, approximate at 48.751 km^2, indicating a rapid urban expansion of Beijing in the 2000s, especially before the 2008 Beijing Olympics. There is a slightly increasing trend of in mean warm-season precipitation over the whole Beijing area from 1980-2000, fluctuating with an increment of 1.033 mm per year. Such a trend is more pronounced from

2000-2012, fluctuating with a linear variation of 12.213 mm per year, whereas such an increasing trend of warm-season precipitation for the UA is more evident (increasing at a rate of 2.077 mm per year from 1980-2000, and 20.633 mm per year from 2000-2012).

Short-duration heavy precipitation events have been occurring more frequently in Beijing during the past few years [*You et al.*, 2014; *Zhang and You*, 2013]. For instance, the heaviest precipitation in 60 years occurred on July 21, 2012, with a record-breaking amount of 460 mm in 18 hours and maximum hourly rainfall rates in excess of 85 mm [*Huang et al.*, 2014; *Wang et al.*, 2013; *Zhang et al.*, 2013a]. *Zheng et al.* [2013] found that the frequency of extreme precipitation events gradually decreased from west to east from 1971-2010, and that the impact of urbanization on precipitation intensity and frequency of extreme precipitation events had become even more apparent. A similar assessment was also provided by *Li and Ma* [2011]. *Yang et al.* [2014] investigated the climatology of summer heavy rainfall events over the Beijing area, confirming that there are two hot spots of higher frequency of summer heavy rainfall events, including the urban core region and the climatological downwind region. However, our findings showed that, although there was an obvious decline in precipitation amount, mean hourly precipitation intensity did not exhibit a significant trend from 1980-2012. Nonetheless, there is an increasing trend at a rate of 0.1 mm/h per year during the 2000-2012 period (which saw especially rapid urban expansion) in the UA (see Figure 10). That trend was more pronounced in the ISAS, fluctuating with a linear variation of 0.16 mm/h per year. We also found that the maximum 1hr precipitation increased from 1980-2012, especially in the transition zone, where the mountains meet the plains area and the UA (see Figures 9 and 11).

It should also be noted that urban heat island effects also constitute an important factor. In urbanized areas, sizeable quantities of anthropogenic heat are generated by human activities [*Zhang* *et al.*, 2013b]. Moreover, growing energy consumption exacerbates local environmental problems, as well as reinforcing temperature increases in the urban atmosphere. Furthermore, the radiative properties of the urban environment are distinctly different, allowing the absorption of additional radiation due to the nature of the urban canopy [*Aikawa et al.*, 2009]. Such changes in the surface heat budget produce atmospheric conditions in urbanized areas that are quite different from those in rural areas, and significantly impact local air circulation and patterns of precipitation [*Huong and Pathirana*, 2013]. *Zhang et al.* [2009] found that urban expansion produces less evaporation, higher surface temperatures, larger sensible heat fluxes, and a deeper boundary layer, which leads to less water vapor, more mixing of water vapor in the boundary layer, and reduces precipitation in Beijing. In our analysis, the effect of urbanization on precipitation intensity has manifested itself in a slightly increasing trend in the mean hourly precipitation intensity and maximum 1hr precipitation intensity in the urban areas. Several other causal factors are known to exist such as large surface roughness and higher aerosol concentration, but their impacts could not be examined in this study because of the lack of data for the Beijing metropolitan area.

5 Implication for water crises

Beijing is already well known as one of the world's most water-challenged cities because of its enormous urban population (more than 20 million) and relatively low average precipitation (averaging about 585 mm during 1950-2012). In comparison, Shanghai, a city with a population 25% larger than Beijing, has an annual precipitation of 1,150 mm (1950-2010 average). Given our finding that precipitation has significantly decreased in Beijing since the 1950s, this trend increasingly exacerbates the city's water shortage, in particular, capita water availability has declined from about

1,000 m^3 in 1949 to 100 m^3 in 2009. Certainly, drought further intensifies this water crisis - Beijing has endured 30 years of below-average precipitation since the 1980s and 13 consecutive dry years from 1999-2011). For example, the Guanting Reservoir currently receives only a fraction of the water it received in the 1950s, and the inflow of the Miyun Reservoir has been steadily declining over the past 20 years (see Figure 13). More specifically, the Guanting Reservoir received 99% less water in 2012 compared to the 1950s, with rivers now dry for most of the year downstream of the reservoir. To cover the supply deficit, unprecedented amounts of ground water are pumped to the surface and now accounts for more than two-thirds of the entire water supply. It is not surprising that this massive ground-water extraction is occurring at a pace faster than it can be recharged, resulting in a sharp drop in the ground-water table (see Figure 13). A report by the *Probe International Beijing Group* [2008] stated that an estimated six billion cubic meters of groundwater above the safe limit have been extracted and may never be replenished. A particular concern is that on a rising number of occasions water supplied from rivers (e.g., the Yongding River) and reservoirs (e.g., the Guanting reservoir) needed to be temporarily abandoned as a source of drinking water because of deteriorating water quality and pollution [*Bao and Fang*, 2012], resulting in the exacerbation of intense water scarcity in the Beijing area.

The Chinese government's main response to Beijing's water crisis is to expand the supply by tapping ever-deeper groundwater, diverting surface-water resources via the massive South-North Water Diversion, accelerating and sea-water desalination, increasing the use of reclaimed water, shutting down or relocating polluting and water-intensive factories, and restricting the water use in neighboring provinces. Since open-ended supply expansion is not a permanent solution of the water crisis, other measures also need to be pursued. For example, water conservation in industry and agriculture can compensate for these losses and free up more water for residential uses. Water charges can be increased to provide an incentive to curb residential water use (efforts to date have been quite limited). Institutional reforms to promote integrated management of water systems have been undertaken recently and need to be expanded. They include restructuring water consumption and water-use patterns (see Figure 14).

[Figure 13 and Figure 14 should be inserted here]

Changes in global and local climate can affect regional water resources by altering the amount and distribution of precipitation in a given area [*Labat et al.*, 2004]. In this regard, urban areas are emerging as “first responders” to accommodate and mitigate climate change [*Mishra et al.*, 2012; *Rosenzweig et al.*, 2010]. Changes in extreme precipitation may pose challenges for urban storm-water management, because existing facilities were designed under the assumption of climate stationarity [*Milly et al.*, 2008]. Another consequence of the increase in extreme precipitation events is widening damage caused by floods [*Roy*, 2009]. Statistics published by the Beijing Hydrological Stations of the Beijing Water Authority show that 37 local heavy precipitation events (those with maximum 1hr precipitation intensities greater than 70mm) occurred in metropolitan Beijing during the period of 2004-2012. These events heighten the possibility of urban flooding, which is aggravated by an outdated urban drainage system than cannot handle the discharges, therefore requiring the modernization and redesign of these facilities [*Zawilski and Brzezińska*, 2013]. A tendency of more intense precipitation has been predicted, and serious problems for urban drainage are expected in the near future. The contradiction or non-conformity between the frequency of precipitation intensity in a changing environment and design standards of urban drainage systems may be an important reason for the increasing world-wide urban flood and inundation in recent years, especially for those cities in developing countries. Beijing's drainage system also has some fundamental flaws because its original designs prioritized the importance of roads and buildings, rather than actual drainage needs. Generally, the design of urban drainage systems is mostly based on precipitation and corresponding storm-water discharge, with certain return periods ranging from 5 to 100 years [*Mishra et al.*, 2012]. However, such design in Beijing is based on precipitation with return periods of around three years (sources: Beijing Water Authority), which is lower than that of many large metropolitan areas, including New York, Tokyo, Paris, and London. This low design standard may be another major cause of heightened urban flooding in recent years. Hence, the Beijing municipal government proposed many additional structural measures to modify the drainage system to handle flood events of return intervals between 3-10 years. Moreover, because urban drainage catchments are relatively small and marked by substantial impervious or semi-pervious surfaces, their response times to extreme precipitation are usually short. Therefore, the intensity and durations of precipitation are both key factors for urban drainage network design [*Li et al.*, 2008; *Wang et al.*, 2012b; *Yin et al.*, 2011]. Both factors can be significantly affected by further urbanization and expansion of the impervious areas in the future.

6. Conclusions

This study has investigated trends in the spatio-temporal variation of precipitation patterns in the Beijing metropolitan area using both the long-time series of annual precipitation during the period 1950-2012 and the relatively short-time series of daily precipitation at 43 rain gauges from 1980-2012. Based on our analysis, we draw the following conclusions:

1) Within the Beijing metropolis, annual precipitation has significantly decreased from 1950-2012

(by almost 32%). Seasonally, a higher decrease in precipitation occurred in the summer and warm season, with a slight increase in spring and autumn precipitation. However, this increase is unable to offset the remarkable decrease in summer and warm-season precipitation, which is the main source of the decline in mean annual precipitation.

2) In general, precipitation in the plains areas is greater than that in the mountainous areas of the metropolis, with the highest values occurring in the northeastern part near the Miyun and Huairou reservoirs. A secondary peak is noted in the eastern part of the outer suburb area.

3) Except for a single sub-region (SWMA), slightly increasing trends to decreasing trends in hourly mean precipitation intensity and maximum 1hr precipitation intensity were observed during the warm season in Beijing, and the changing point occurred at the end of the 1990s and the beginning of the 2000s. Similar to the warm-season precipitation during the same period, there are two hot spots of greater incidence of mean hourly precipitation intensity and maximum 1hr precipitation. One hot spot is located in the central urban area, and the other is located in the topographic transition zone in the northeast.

4) Changes in Beijing's precipitation are influenced by many factors, which include local climate conditions, topographical effect, and the expanding urban landscape. The amount and intensity of precipitation in the plains areas is greater than in the mountainous areas, and precipitation in the urban areas is relatively greater than in the suburb areas.

5) Decreasing precipitation amounts in Beijing, especially around the Miyun Reservoir in the northeast, will worsen the already troubled local water supply. In the mean time, higher precipitation intensity elevates the risk of urban flooding [*Wang et al.*, 2013; *You et al.*, 2014]. All of these factors pose new and severe challenges for water-resources management under the

growing impact of climate change and human activities.

Acknowledgements

Rainfall data to support this article are available from the Hydrological Data of Haihe River Baisn (in Chinese), the Annual Hydrological Report of China (Volume: III), released by Ministry of Water Resources of China. For further information or right to access to the material used in this paper, readers can also contact the Beijing Hydrological Center (http://www.bjswzz.com/) of the Beijing Water Authority (http://www.bjwater.gov.cn/pub/bjwater/index.html). Weather data supporting Figure 12a are available as in Supporting Information Table S1. For annual precipitation, urban development and water resources data used in this article, readers can contact the corresponding author X. Song. This study was supported by the National Basic Research Program of China (2010CB951103), the Postgraduate Dissertation Foundation of the Nanjing Hydraulic Research Institute (LB51302), and the National Natural Science Foundation of China (L1322014, 41330854, 41371063, and 51309155). We are thankful to the Beijing Hydrological Stations, Beijing Water Authority for providing the precipitation data. We are also grateful to Prof. Xuesong Zhang, Pacific Northwest National Laboratory and University of Maryland for his suggestions. We also thank the editor Prof. L. Ruby Leung and three anonymous reviewers for their constructive suggestions and comments, which were most helpful in improving this article. We are also very grateful to Dr. Peter Muller for all the editorial suggestions he made for significantly improving the paper.

References

Aikawa, M., T. Hiraki, and J. Eiho (2009), Change of atmospheric condition in an urbanized area of Japan from the viewpoint of rainfall intensity, *Environ Monit Assess*, *148*(1-4), 449-453, doi:10.1007/s10661-008-0174-0.

Alexander, L. V., et al. (2006), Global observed changes in daily climate extremes of temperature and precipitation, *Journal of Geophysical Research*, *111*(D5), doi:10.1029/2005jd006290.

Allamano, P., P. Claps, F. Laio, and C. Thea (2009), A data-based assessment of the dependence of short-duration precipitation on elevation, *Physics and Chemistry of the Earth*, *34*(10-12), 635-641, doi:10.1016/j.pce.2009.01.001.

Bao, C., and C.-l. Fang (2012), Water Resources Flows Related to Urbanization in China: Challenges and Perspectives for Water Management and Urban Development, *Water Resources Management*, *26*(2), 531-552, doi:10.1007/s11269-011-9930-y.

Bao, Z., J. Zhang, G. Wang, G. Fu, R. He, X. Yan, J. Jin, Y. Liu, and A. Zhang (2012), Attribution for decreasing streamflow of the Haihe River basin, northern China: Climate variability or human activities?, *Journal of Hydrology*, *460-461*, 117-129, doi:10.1016/j.jhydrol.2012.06.054.

Berne, A., G. Delrieu, J. Creutin, and C. Obled (2004), Temporal and spatial resolution of rainfall measurements required for urban hydrology, *Journal of Hydrology*, *299*(3-4), 166-179, doi:10.1016/S0022-1694(04)00363-4|10.1016/j.jhydrol.2004.08.002.

Chu, H. (2012), Assessing the relationships between elevation and extreme precipitation with various durations in southern Taiwan using spatial regression models, *Hydrological Processes*, *26*(21), 3174-3181, doi:10.1002/hyp.8403.

Chu, J., J. Xia, C. Xu, L. Li, and Z. Wang (2010), Spatial and temporal variability of daily precipitation in Haihe River basin, 1958–2007, *Journal of Geographical Sciences*, *20*(2), 248-260, doi:10.1007/s11442-010-0248-0.

Chu, M. L., J. H. Knouft, A. Ghulam, J. A. Guzman, and Z. Pan (2013), Impacts of urbanization on river flow frequency: A controlled experimental modeling-based evaluation approach, *Journal of Hydrology*, *495*, 1-12, doi:10.1016/j.jhydrol.2013.04.051.

Cong, Z., J. Zhao, D. Yang, and G. Ni (2010), Understanding the hydrological trends of river basins in China, *Journal of Hydrology*, *388*(3-4), 350-356, doi:10.1016/j.jhydrol.2010.05.013.

Creamean, J. M., et al. (2013), Dust and biological aerosols from the Sahara and Asia influence precipitation in the western U.S, *Science*, *339*(6127), 1572-1578, doi:10.1126/science.1227279.

Dai, A. (2013), Increasing drought under global warming in observations and models, *Nature Climate Change*, *3*(1), 52-58, doi:10.1038/nclimate1633.

Damberg, L., and A. AghaKouchak (2014), Global Trends and Patterns of Droughts from Space, *Theor. Appl. Climatol.*, doi:10.1007/s00704-013-1019-5.

Du, J. K., L. Qian, H. Y. Rui, T. H. Zuo, D. P. Zheng, Y. P. Xu, and C. Y. Xu (2012), Assessing the effects of urbanization on annual runoff and flood events using an integrated hydrological modeling system for Qinhuai River basin, China, *Journal of Hydrology*, *464*, 127-139, doi:10.1016/j.jhydrol.2012.06.057.

Fletcher, T. D., H. Andrieu, and P. Hamel (2013), Understanding, management and modelling of urban hydrology and its consequences for receiving waters: A state of the art, *Advances in Water Resources*, *51*, 261-279, doi:10.1016/j.advwatres.2012.09.001.

Ganeshan, M., R. Murtugudde, and M. L. Imhoff (2013), A multi-city analysis of the UHI-influence on warm season rainfall, *Urban Climate*, *6*, 1-23, doi:10.1016/j.uclim.2013.09.004.

Garen, D., and D. Marks (2005), Spatially distributed energy balance snowmelt modelling in a mountainous river basin: estimation of meteorological inputs and verification of model results, *Journal of Hydrology*, *315*(1-4), 126-153, doi:10.1016/j.jhydrol.2005.03.026.

Grimm, N. B., S. H. Faeth, N. E. Golubiewski, C. L. Redman, J. Wu, X. Bai, and J. M. Briggs (2008), Global change and the ecology of cities, *Science*, *319*(5864), 756-760, doi:10.1126/science.1150195.

Han, J.-Y., J.-J. Baik, and H. Lee (2014a), Urban impacts on precipitation, *Asia-Pacific Journal of Atmospheric Sciences*, *50*(1), 17-30, doi:10.1007/s13143-014-0016-7.

Han, J. Y., and J. J. Baik (2008), A theoretical and numerical study of urban heat island-induced circulation and convection, *Journal of the Atmospheric Sciences*, *65*(6), 1859-1877, doi:10.1175/2007JAS2326.1.

Han, Z., Z. Yan, Z. Li, W. Liu, and Y. Wang (2014b), Impact of urbanization on low-temperature precipitation in Beijing during 1960–2008, *Advances in Atmospheric Sciences*, *31*(1), 48-56, doi:10.1007/s00376-013-2211-3.

Hao, Z., A. AghaKouchak, and T. J. Phillips (2013), Changes in concurrent monthly precipitation and temperature extremes, *Environmental Research Letters*, *8*(3), 034014, doi:10.1088/1748-9326/8/3/034014.

Hao, L., J. Min, and X. Yao (2007), Analysis on the causes resulting in the reduction of summer rainfall over North China, Arid Zone Research, 24(4), 522-527. (in Chinese)

Hao, L., J. Min, and Y. Ding (2011). Analysis of precipitation events changes and causes for rainstorm events reduction in North China. Chinese J. Geophys., 54(5), 1160-1167. doi: 10.3969/j.issn.0001-5733.2011.05.003

Huang, Y., et al. (2014), Evaluation of Version-7 TRMM Multi-Satellite Precipitation Analysis Product during the Beijing Extreme Heavy Rainfall Event of 21 July 2012, *Water*, *6*(1), 32-44, doi:10.3390/w6010032.

Huong, H. T. L., and A. Pathirana (2013), Urbanization and climate change impacts on future urban flooding in Can Tho city, Vietnam, *Hydrology and Earth System Sciences*, *17*(1), 379-394, doi:10.5194/hess-17-379-2013.

Jackson, C. R. (2011), Identification and quantification of the hydrological impacts of imperviousness in urban catchments: A review, *Journal of Environmental Management*, *92*(6), 1438-1448, doi:10.1016/j.jenvman.2011.01.018.

Kaufmann, R. K., K. C. Seto, A. Schneider, Z. Liu, L. Zhou, and W. Wang (2007), Climate Response to Rapid Urban Growth: Evidence of a Human-Induced Precipitation Deficit, *Journal of Climate*, *20*(10), 2299-2306, doi:10.1175/jcli4109.1.

Kendall, M. G. (1975), Rank correlation methods, Griffin, Londn, UK

Labat, D., Y. Goddéris, J. L. Probst, and J. L. Guyot (2004), Evidence for global runoff increase related to climate warming, *Advances in Water Resources*, *27*(6), 631-642, doi:10.1016/j.advwatres.2004.02.020.

Ladson, A. R., C. J. Walsh, and T. D. Fletcher (2006), Improving stream health in urban areas by reducing runoff frequency from impervious surfaces, *Australian Journal of Water Resources*, *10*(1), 23-33.

Li, J., R. Yu, and J. Wang (2008), Diurnal variations of summer precipitation in Beijing, *Chinese Science Bulletin*, *53*(12), 1933-1936, doi:10.1007/s11434-008-0195-7.

Li, S. Y., and J. J. Ma (2011), Impact of urbanization on precipitation in Beijing area, *Journal of the Meteorological Sciences*, *31*(4), 414-421.

Li, W., S. Chen, G. Chen, W. Sha, C. Luo, Y. Feng, Z. Wen, and B. Wang (2011), Urbanization signatures in strong versus weak precipitation over the Pearl River Delta metropolitan regions of China, *Environmental Research Letters*, *6*(3), 034020, doi:10.1088/1748-9326/6/3/034020.

Li, X., W. Zhou, and Z. Ouyang (2013), Forty years of urban expansion in Beijing: What is the relative importance of physical, socioeconomic, and neighborhood factors?, *Applied Geography*, *38*, 1-10, doi:10.1016/j.apgeog.2012.11.004.

Liang, L., L. Li, and Q. Liu (2011a), Precipitation variability in Northeast China from 1961 to 2008, *Journal of Hydrology*, *404*(1-2), 67-76, doi:10.1016/j.jhydrol.2011.04.020.

Liang, L. J., Z. S. Yang, and G. Y. Bai (2011b), Discussion on influence of urbanization on precipitation in Beijing, *Beijing Water*(3), 15-18.

Liu, B., M. Xu, M. Henderson, and Y. Qi (2005), Observed trends of precipitation amount, frequency, and intensity in China, 1960–2000, *Journal of Geophysical Research*, *110*(D8), doi:10.1029/2004JD004864.

Lloyd, C. (2005), Assessing the effect of integrating elevation data into the estimation of monthly precipitation in Great Britain, *Journal of Hydrology*, *308*(1-4), 128-150, doi:10.1016/j.jhydrol.2004.10.026.

Luce, C., J. Abatzoglou, and Z. Holden (2013), The Missing Mountain Water: Slower Westerlies Decrease Orographic Enhancement in the Pacific Northwest USA, *Science*, *342*(6164), 1360-1364, doi:10.1126/science.1242335.

Mann, H. B. (1945), Nonparametric tests against trend, *Econometrica*, 13, 245-259

Miao, S. G., F. Chen, M. A. Lemone, M. Tewari, Q. C. Li, and Y. C. Wang (2009), An Observational and Modeling Study of Characteristics of Urban Heat Island and Boundary Layer Structures in Beijing, *J. Appl. Meteorol. Climatol.*, *48*(3), 484-501, doi:10.1175/2008jamc1909.1.

Miao, S. G., F. Chen, Q. C. Li, and S. Y. Fan (2011), Impacts of urban processes and urbanization on summer precipitation: A case study of heavy rainfall in Beijing on 1 August 2006, *J. Appl. Meteorol. Climatol.*, 50(4): 806-825, doi: 10.1175/2010JAMC2513.1

Miller, M. D. (2012), The impacts of Atlanta's urban sprawl on forest cover and fragmentation, *Appl. Geogr.*, *34*, 171-179, doi:10.1016/j.apgeog.2011.11.010.

Milly, P. C., J. Betancourt, M. Falkenmark, R. M. Hirsch, Z. W. Kundzewicz, D. P. Lettenmaier, and R. J. Stouffer (2008), Stationarity is dead: whither water management?, *Science*, *319*(5863), 573-574, doi:10.1126/science.1151915.

Mishra, V., F. Dominguez, and D. P. Lettenmaier (2012), Urban precipitation extremes: How reliable are regional climate models?, *Geophys. Res. Lett.*, *39*(3), doi:10.1029/2011gl050658.

Mosmann, V., A. Castro, R. Fraile, J. Dessens, and J. L. Sánchez (2004), Detection of statistically significant trends in the summer precipitation of mainland Spain, *Atmos. Res.*, *70*(1), 43-53, doi:10.1016/j.atmosres.2003.11.002.

Oke, T. R. (1973), City size and the urban heat island, *Atmos. Environ.*, *7*(8), 769-779, doi:10.1016/0004-6981(73)90140-6.

Oke, T.R., and K. Muusiake (1994), Seasonal change of the diurnal cycle of precipitation over Japan and Malaysia, J. Appl. Meteor., 33, 1445-1463.

Partal, T., and E. Kahya (2006), Trend analysis in Turkish precipitation data, *Hydrol. Process.*, 20, 2011-2026

Pathirana, A., H. B. Denekew, W. Veerbeek, C. Zevenbergen, and A. T. Banda (2014), Impact of urban growth-driven landuse change on microclimate and extreme precipitation — A sensitivity study, *Atmos. Res.*, *138*, 59-72, doi:10.1016/j.atmosres.2013.10.005.

Pinto, O., I. R. C. A. Pinto, and M. A. S. Ferro (2013), A study of the long-term variability of thunderstorm days in southeast Brazil, *Journal of Geophysical Research: Atmospheres*, *118*(11), 5231-5246, doi:10.1002/jgrd.50282.

Probe International Beijing Group (2008), Beijing's water crisis 1949-2008 Olympics, June 2008. http://journal.probeinternational.org/2008/06/26/beijings-water-crisis-1949-2008-olympics/

Ren, G., Y. Zhou, Z. Chu, J. Zhou, A. Zhang, J. Guo, and X. Liu (2008), Urbanization Effects on Observed Surface Air Temperature Trends in North China, *Journal of Climate*, *21*(6), 1333-1348, doi:10.1175/2007jcli1348.1.

Rosenzweig, C., W. Solecki, S. A. Hammer, and S. Mehrotra (2010), Cities lead the way in climate-change action, *Nature*, *467*(7318), 909-911, doi:10.1038/467909a.

Roy, S. S. (2009), A spatial analysis of extreme hourly precipitation patterns in India, *Int. J. Climatol.*, *29*(3), 345-355, doi:10.1002/joc.1763.

Russell, A., and M. Hughes (2012), Is the changing precipitation regime of Manchester, United Kingdom, driven by the development of urban areas?, *International Journal of Climatology*, *32*(6), 967-974, doi:10.1002/joc.2321.

Seto, K. C., M. Fragkias, B. Guneralp, and M. K. Reilly (2011), A meta-analysis of global urban land expansion, *PLoS One*, *6*(8), e23777, doi:10.1371/journal.pone.0023777.

Siler, N., and G. Roe (2014), How will orographic precipitation respond to surface warming? An idealized themodynamic perspective, Geophys. Res. Lett. 41, 2606-2613. doi:10.1002/2013GL059095.

Smith, R. B. (1979), The influence of mountains on the atmosphere, *Adv. Geophys.*, 21, 87-230. DOI: 10.1016/S0065-2687(08)60262-9

Sun, J. S., and B. Yang (2008), Meso-β scale torrential rain affected by topography and the urban circulation, *Chinese Journal of Atmospheric Sciences*, *32*(6), 1352-1364.

Tabari, T., B. S. Somee, and M. R. Zadeh (2011), Testing for long-term trends in climatic variables in Iran, *Atmos. Res.*, 100(1), 132-140. DOI: 10.1016/j.atmosres.2011.01.005

United Nations, D. o. E. a. S. A. (2012), World Urbanization Prospects – the 2011 Rivision*Rep.*, New York.

Wang, J., J. Feng, Z. Yan, Y. Hu, and G. Jia (2012a), Nested high-resolution modeling of the impact of urbanization on regional climate in three vast urban agglomerations in China, *Journal of Geophysical Research: Atmospheres*, *117*(D21), n/a-n/a, doi:10.1029/2012JD018226.

Wang, J., R. Zhang, and Y. Wang (2012b), Areal differences in diurnal variations in summer precipitation over Beijing metropolitan region, *Theor. Appl. Climatol.*, *110*(3), 395-408, doi:10.1007/s00704-012-0636-8.

Wang, K., L. Wang, Y.-M. Wei, and M. Ye (2013), Beijing storm of July 21, 2012: observations and reflections, *Natural Hazards*, *67*(2), 969-974, doi:10.1007/s11069-013-0601-6.

Wang, X. Q., Z. F. Wang, Y. B. Qi, and H. Guo (2009), Effect of urbanization on the winter precipitation distribution in Beijing area, *Sci. China Ser. D-Earth Sci.*, *52*(2), 250-256, doi:10.1007/s11430-009-0019-x.

Wang, X., W. Wang, H. Liu, and H. Wang (2008), Beijing region precipitation feature and some statistics of relationship between it and SHWP, Plateau Meteorology, 27(4), 822-829. (in Chinese)

Westra, S., L. V. Alexander, and F. W. Zwiers (2013), Global Increasing Trends in Annual Maximum Daily Precipitation, *Journal of Climate*, *26*(11), 3904-3918, doi:10.1175/jcli-d-12-00502.1.

Wu, X. (2012), Beijing urban impervious surface space-time pattern analysis and planning applications, Hohhot city.

Xu, M., C.-P. Chang, C. Fu, Y. Qi, A. Robock, D. Robinson, and H.-m. Zhang (2006a), Steady decline of east Asian monsoon winds, 1969–2000: Evidence from direct ground measurements of wind speed, *Journal of Geophysical Research*, *111*(D24), doi:10.1029/2006jd007337.

Xu, Y., S. Liu, F. Hu, N. Ma, Y. Wang, Y. Shi, H. Jia (2009) Influence of Beijing urbanization on the characteristics of atmospheric boundary layer. *Chinese Journal of Atmospheric Sciences*, 33(4), 859-867. (in Chinese)

Xu, Z. X., L. Zhang, and B. Q. Ruan (2006b), Analysis on the spatio-temporal distribution of precipitation in the Beijing region, *Arid Land Geography*, *29*(2), 186-192.

Yang, F. L., and K. M. Lau (2004), Trend and variability of China precipitation in spring and summer: Linkage to sea-surface temperatures, *International Journal of Climatology*, *24*(13), 1625-1644, doi:10.1002/joc.1094.

Yang, G., L. C. Bowling, K. A. Cherkauer, and B. C. Pijanowski (2011), The impact of urban development on hydrologic regime from catchment to basin scales, *Landscape and Urban Planning*, *103*(2), 237-247, doi:10.1016/j.landurbplan.2011.08.003.

Yang, L., F. Tian, J. A. Smith, and H. Hu (2014), Urban signatures in the spatial clustering of summer heavy rainfall events over the Beijing metropolitan region, *Journal of Geophysical Research: Atmospheres*, *119*(3), 1203-1217, doi:10.1002/2013JD020762.

Yang, P., G. Ren, W. Hou, and W. Liu (2013), Spatial and diurnal characteristics of summer rainfall over Beijing Municipality based on a high-density AWS dataset, *Int. J. Climatol.*, *33*(13), 2769-2780, doi:10.1002/joc.3622.

Yin, S., W. Li, D. Chen, J.-H. Jeong, and W. Guo (2011), Diurnal variations of summer precipitation in the Beijing area and the possible effect of topography and urbanization, *Advances in Atmospheric Sciences*, *28*(4), 725-734, doi:10.1007/s00376-010-9240-y.

You, H., W. Liu, and G. Ren (2014), Variation characteristics of precipitation extremes in Beijing during 1981-2010, *Climatic and Environmental Research*, *19*(1), 69-77, doi:10.3878/j.issn.1006-9585.2012.12143.

Zawilski, M., and A. Brzezińska (2013), Areal rainfall intensity distribution over an urban area and its effect on a combined sewerage system, *Urban Water Journal*, 1-11, doi:10.1080/1573062x.2013.831909.

Zhai, P., X. Zhang, H. Wan, and X. Pan (2005), Trends in Total Precipitation and Frequency of Daily Precipitation Extremes over China, *Journal of Climate*, *18*(7), 1096-1108, doi:10.1175/jcli-3318.1.

Zhai, Y., Y. Guo, J. Zhou, N. Guo, J. Wang, and Y. Teng (2014), The spatio-temporal variability of annual precipitation and its local impact factors during 1724-2010 in Beijing, China, *Hydrological Processes*, *28*(4), 2192-2201, doi:10.1002/hyp.9772.

Zhang, C., C. Ji, Y. Kuo, S. Fan, C. Xuan, and M. Chen (2005), Numerical simulation of topography effects on the "00.7" server rainfall in Beijing, *Progress in Natural Science*, *15*(9), 818-826, doi:10.1080/10020070512331342970.

Zhang, C. L., F. Chen, S. G. Miao, Q. C. Li, X. A. Xia, and C. Y. Xuan (2009), Impacts of urban expansion and future green planting on summer precipitation in the Beijing metropolitan area, *J. Geophys. Res.-Atmos.*, *114*, 26, doi:10.1029/2008jd010328.

Zhang, D.-L., Y. Lin, P. Zhao, X. Yu, S. Wang, H. Kang, and Y. Ding (2013a), The Beijing extreme rainfall of 21 July 2012: "Right results" but for wrong reasons, *Geophys. Res. Lett.*, *40*(7), 1426-1431, doi:10.1002/grl.50304.

Zhang, J., and H. You (2013), Study on Changes of Precipitation Extremes in Beijing, *Climate Change Research Letters*, *02*(04), 131-136, doi:10.12677/ccrl.2013.24022.

Zhang, Q., V. P. Singh, J. Li, and X. Chen (2011), Analysis of the periods of maximum consecutive wet days in China. *J. Geophys. Res.*, *116*, D23106, doi:10.1029/2011JD016088.

Zhang, Q., V. P. Singh, J. Peng, Y. D. Chen, and J. Li (2012), Spatial–temporal changes of precipitation structure across the Pearl River basin, China, *Journal of Hydrology*, *440-441*, 113-122, doi:10.1016/j.jhydrol.2012.03.037.

Zhang, X., H. Wan, F. W. Zwiers, G. C. Hegerl, and S.-K. Min (2013b), Attributing intensification of precipitation extremes to human influence, *Geophys. Res. Lett.*, *40*(19), 5252-5257, doi:10.1002/grl.51010.

Zhang, Y., J. A. Smith, L. Luo, Z. Wang, and M. L. Baeck (2014), Urbanization and rainfall variability in the Beijing metropolitan region, *Journal of Hydrometeorology*, in press, doi: 10.1175/JHM-D-13-0180.1

Zheng, S. Y., and S. H. Liu (2008), Urbanization effect on climate in Beijing, *Climatic and Environmental Research*, *13*(2), 123-133.

Zheng, Z., Z. Wang, and H. Gao (2013), Characteristics of extreme precipitation events in summer and its effect on urbanization in Beijing area, *Meteorological Monthly*, *39*(12), 1635-1641, doi:10.7519/j.issn.1000-0526.2013.12.012.

Zhong, Y., Y. Jia, and Z. Li (2013), Spatial and temporal changes of maximum 1h precipitation intensity in Beijing region in last 53 years, *Journal of China Hydrology*, *33*(1), 32-37.

Zhu, L., Y. Chen, R. Yan, T. Shen, L. Jiang, and Y. Wang (2012), Characteristics of precipitation and temperature changes in Beijing city during 1951-2010, *Resource Science*, *34*(7), 1287-1297.

Figures and Tables

Figure 1. The location and topography map of Beijing and the 43 rain gauges in Beijing. Red solid lines denote the boundaries of the six areas. UA, ISAS, ISAN, OSA, NWMA, and SWMA refer to the urban area, inner suburb area in south, inner suburb area in north, outer suburb area, northwestern mountainous area, and southwestern mountainous area, respectively.

Figure 2. The time series of mean precipitation from 1950-2012 in the Beijing area in (a) spring (March, April, and May), (b) summer (June, July, and August), (c) autumn (September, October and November), (d) winter (December, January and February), (e) warm season (June to September), (f) annual.

Figure 3. Box plots of the decadal-average precipitation from 1950-2012 in (a) spring, (b) summer, (c) autumn, (d) winter, (e) warm season and (f) annual. The square marks represent the mean value of precipitation data. The top, middle and bottom horizontal line represent the 75th percentile, median and the 25th percentile, respectively. The solid and hollow circles represent the maximum and minimum values.

Figure 4. M-K test statistic results of the annual mean precipitation and seasonal mean precipitation from 1950-2012: (a) spring, (b) summer, (c) autumn, (d) winter, (e) warm season, (f) annual. Dashed lines are the confidence limits at the 95% confidence level.

Figure 5 (a) Percentage contributions of monthly precipitation to the annual precipitation amount, and (b) annual cycle of mean precipitation for different periods over the Beijing area

Figure 6. Distribution of decadal-averaged warm-season precipitation (mm) in the Beijing area: (a) from 1980-1989 (1980s), (b) 1990-1999 (1990s), (c) 2000-2009 (2000s), and the differences of precipitation for the three decades: (d) between 1980s and 1990s, (e) between 1990s and 2000s, (f) between 1980s and 2000s.

Figure 7. Spatial distribution of precipitation trends in the warm season across the Beijing area from 1980-2012. Red triangles represent insignificant increasing trend. Green triangles denote insignificant decreasing trend. Green triangles with black circles show significant decreasing trend at the 95% confidence level. D.T. represents a decreasing trend and a U.T. upward trend.

Figure 8. Time series and Mann-Kendall's test statistics values of the precipitation amount in warm season for different parts of the Beijing area from 1980-2012.

Figure 9. Spatial variation (a and b) and the M-K-based trends (c and d) of precipitation intensity from 1980-2012. Left panel (a and c) represents the hourly mean precipitation intensity, and right panel (b, d) is the maximum 1hr precipitation intensity. PI indicates precipitation intensity.

Figure 10. Time series and the Mann-Kendall test results of mean hourly precipitation intensity in

the warm season for the six areas in the Beijing area during the past three decades

Figure 11. Time series and the Mann-Kendall test results of maximum 1-hour precipitation intensity in the warm season for the six areas in the Beijing area over the past three decades

Figure 12. (a) Mean temperature for Beijing Guanxiangtai weather station from 1951-2012, and (b) warm season precipitation and the urban built-up areas in Beijing from 1980-2012. The meaning of the lines with symbols is illustrated in the lower-left of each plot, and the lines without symbols are their corresponding linear tendency change (see linear-fitted equations).

Figure 13. Variation of surface water availability in the Beijing area: variation of inflow and storage capacity for (a) the Guanting and (b) Miyun reservoirs, and variation of the groundwater table (c) in the plain areas of Beijing and (d) in the districts. CY-Chaoyang, FT-Fengtai, HD-Haidian, SJS-Shijingshan, TZ-Tongzhou, DX-Daxing, FS-Fangshan, MTG-Mengtougou, CP-Changping, SY-Shunyi, YQ-Yanqing, HR-Huairou, MY-Miyun, PG-Pinggu

Figure 14. (a) Changes of water-use structure from 1980-2012 and (b) changes of water-use structure from 2001-2012.

Table 1. Information for all the stations and the six regions in the Beijing area

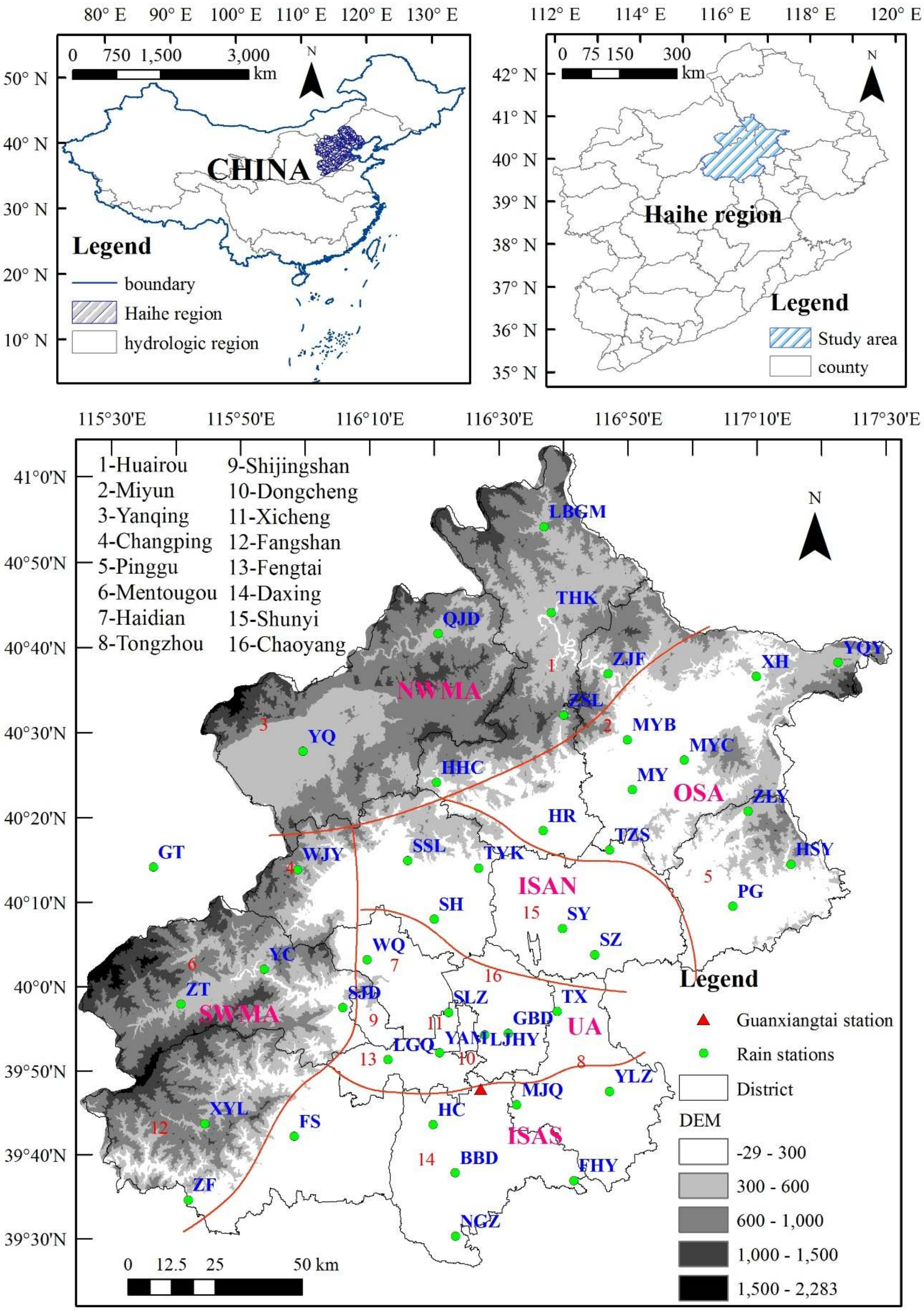

Figure 1. The location and topography map of Beijing and 43 rain gauges in Beijing. Red solid lines denote the boundaries of the six areas. UA, ISAS, ISAN, OSA, NWMA, and SWMA refer to the urban area, inner suburb area in south, inner suburb area in north, outer suburb area, northwestern mountainous area, and southwestern

mountainous area.

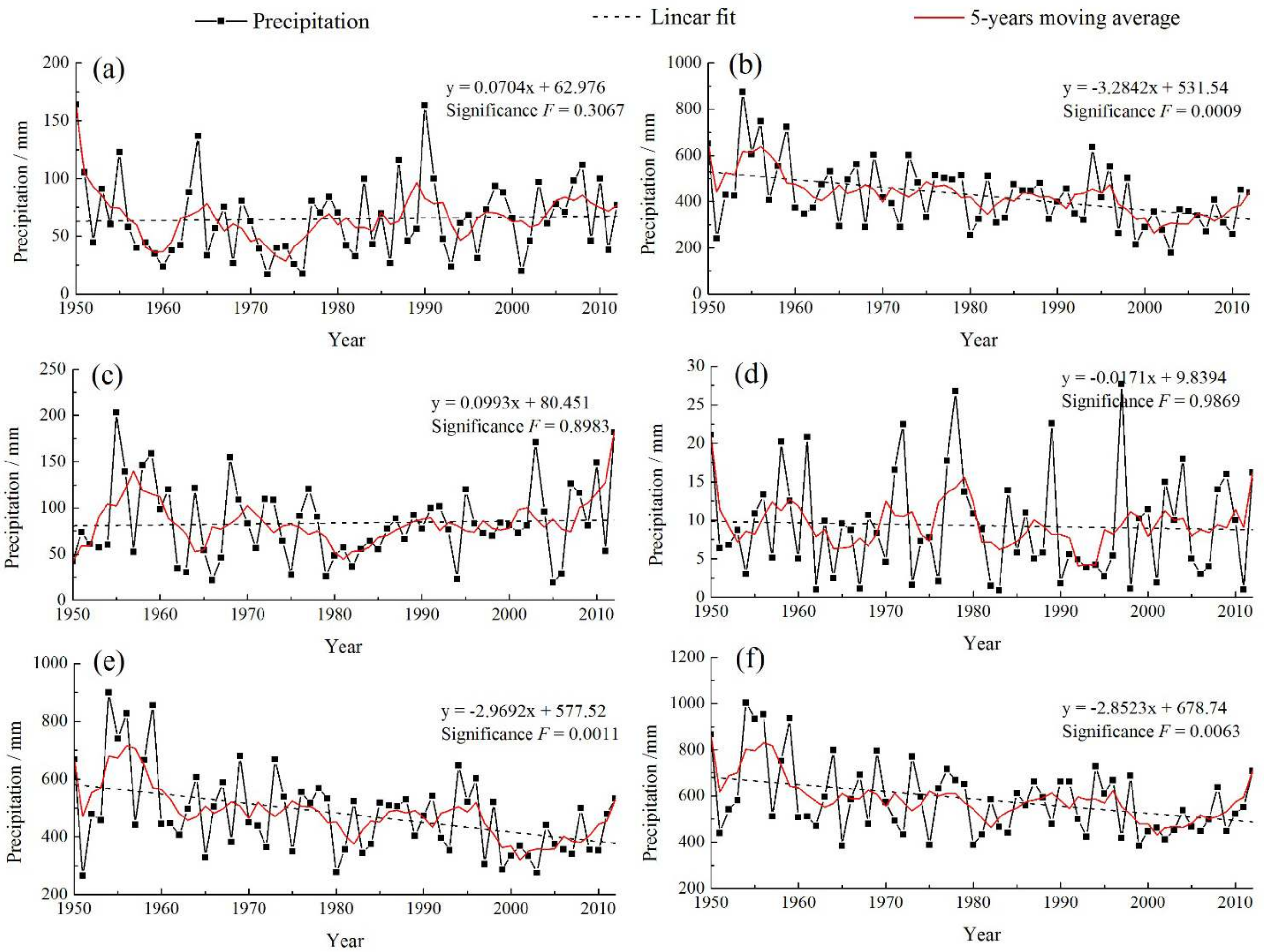

Figure 2. The time series of mean precipitation from 1950-2012 in the Beijing area in (a) spring (March, April, and May), (b) summer (June, July, and August), (c) autumn (September, October and November), (d) winter (December, January and February), (e) warm season (June to September), (f) annual.

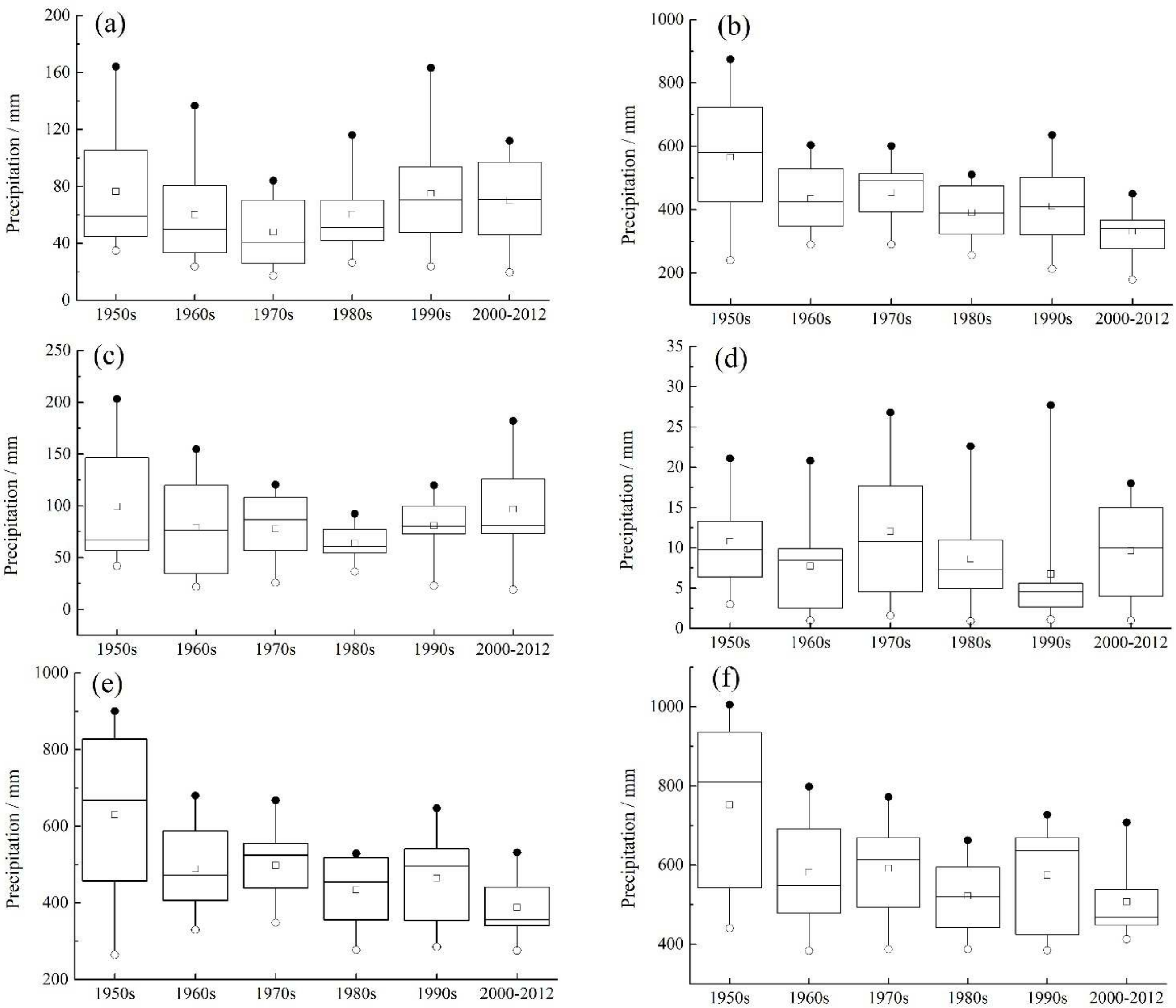

Figure 3. Box chart of the decadal-average precipitation from 1950-2012 in (a) spring, (b) summer, (c) autumn, (d) winter, (e) warm season and (f) annual. Small squares represent the mean value of precipitation data. The top, middle and bottom horizontal line represent the 75th percentile value, median value and the 25th percentile value. The solid and hollow circle represent the maximum and minimum value respectively.

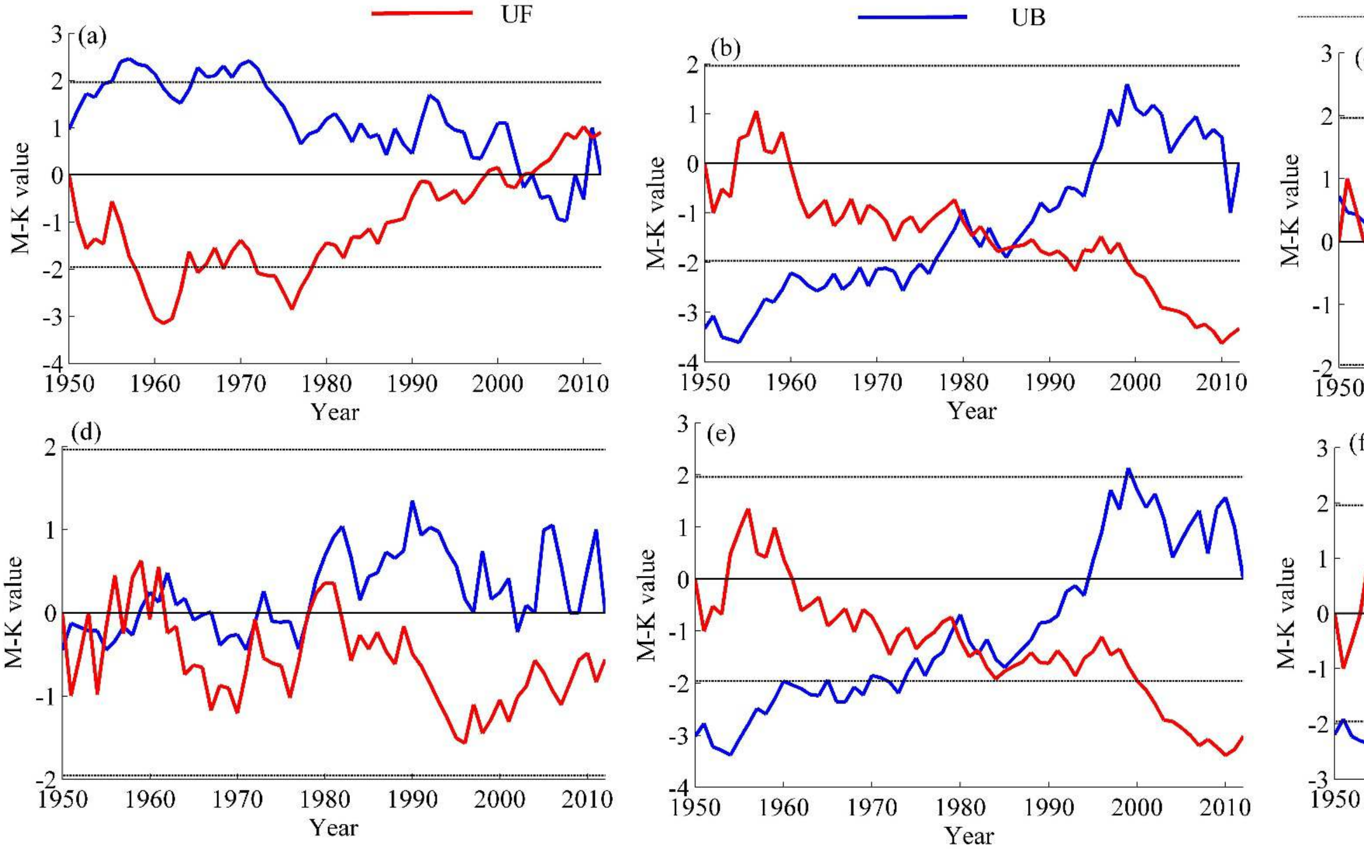

Figure 4. M-K statistical test results of the annual mean precipitation and seasonal mean precipitation from 1950-2012: (a) sp
(e) warm season, (f) annual. Dashed lines are the confidence limits at the 95% confidence level

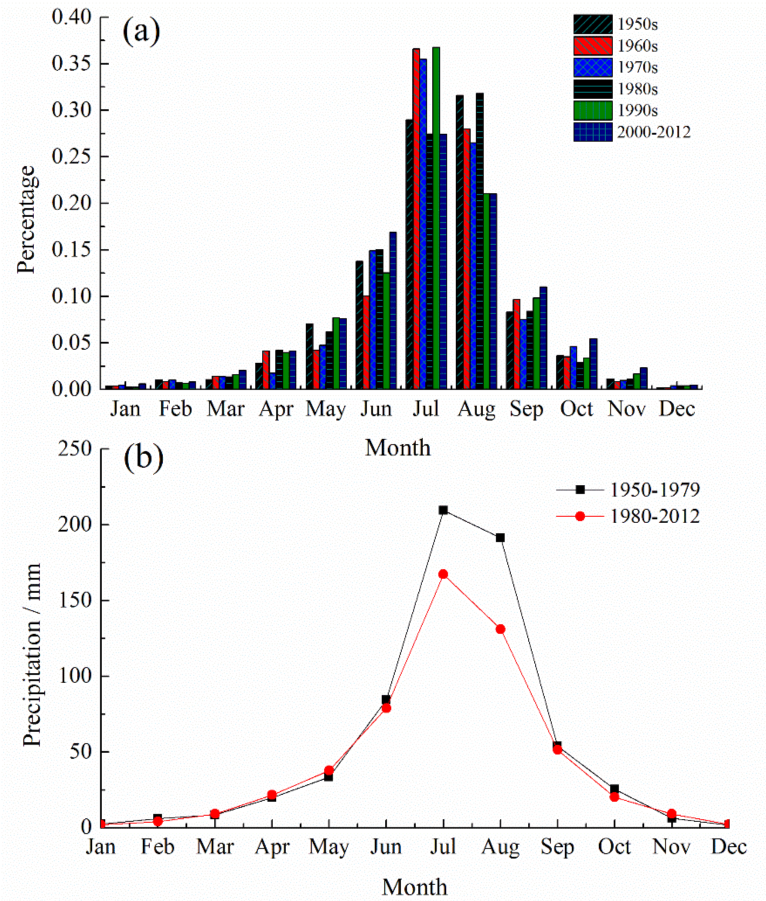

Figure 5 (a) Percentage contributions of monthly precipitation to the annual precipitation amount, and (b) annual cycle of mean precipitation for different periods over the Beijing area

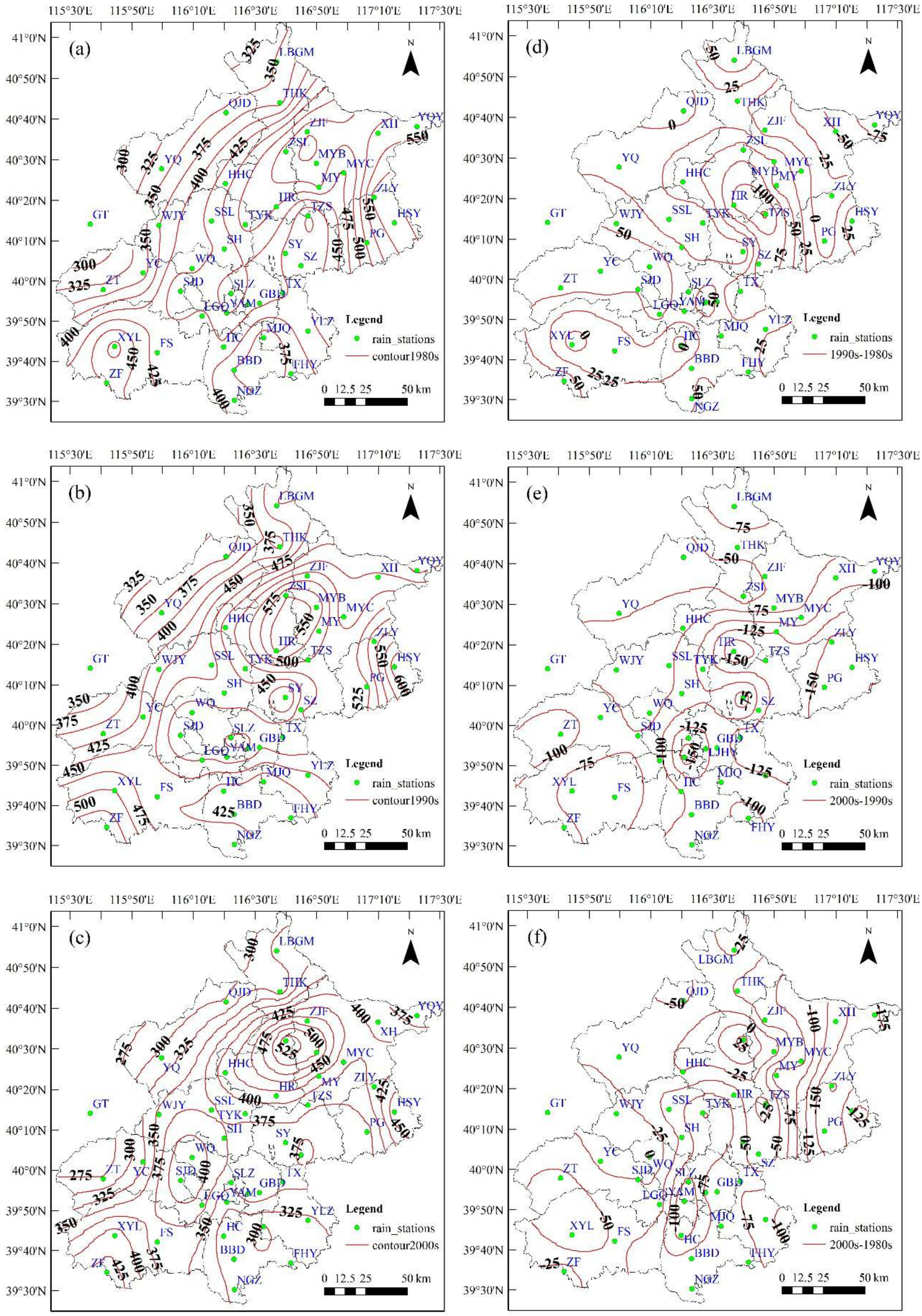

Figure 6. Distribution of decadal-averaged warm-season precipitation (mm) in the Beijing area: (a) for 1980-1989 (1980s), (b) 1990-1999 (1990s), (c) 2000-2009 (2000s), and the differences of precipitation for the three decades: (d) between 1980s and 1990s, (e) between 1990s and 2000s, (f) between 1980s and 2000s.

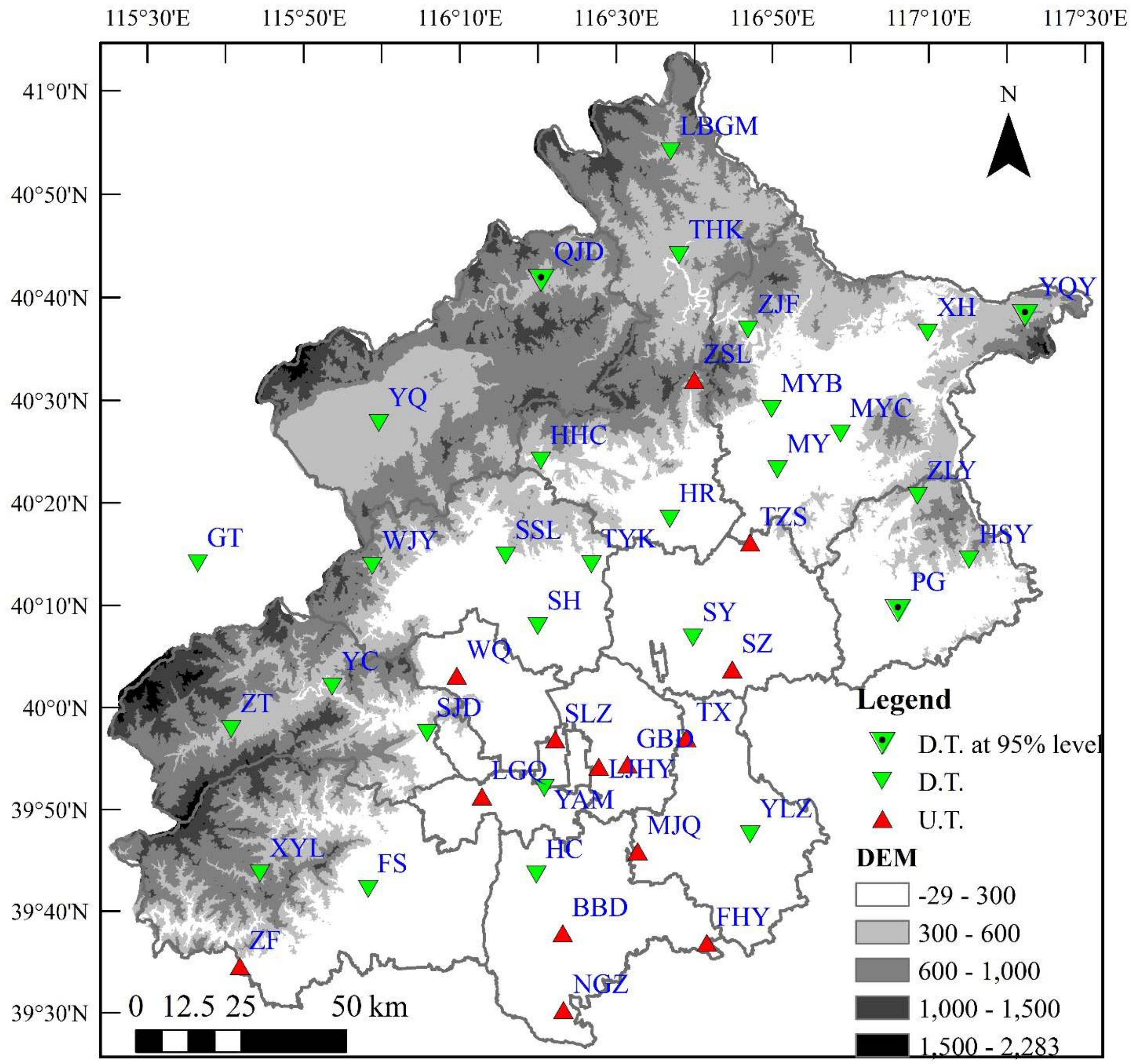

Figure 7. Spatial distribution of trends of precipitation amount in the warm season across the Beijing area during 1980-2012. Red triangle represents the increasing trends with no significant trends. Green triangle denote decreasing trends but with no significant trends. Green triangle with black circle show significant decreasing trends at the 95% confidence level. D.T. represents the decreasing trend and U.T upward trend.

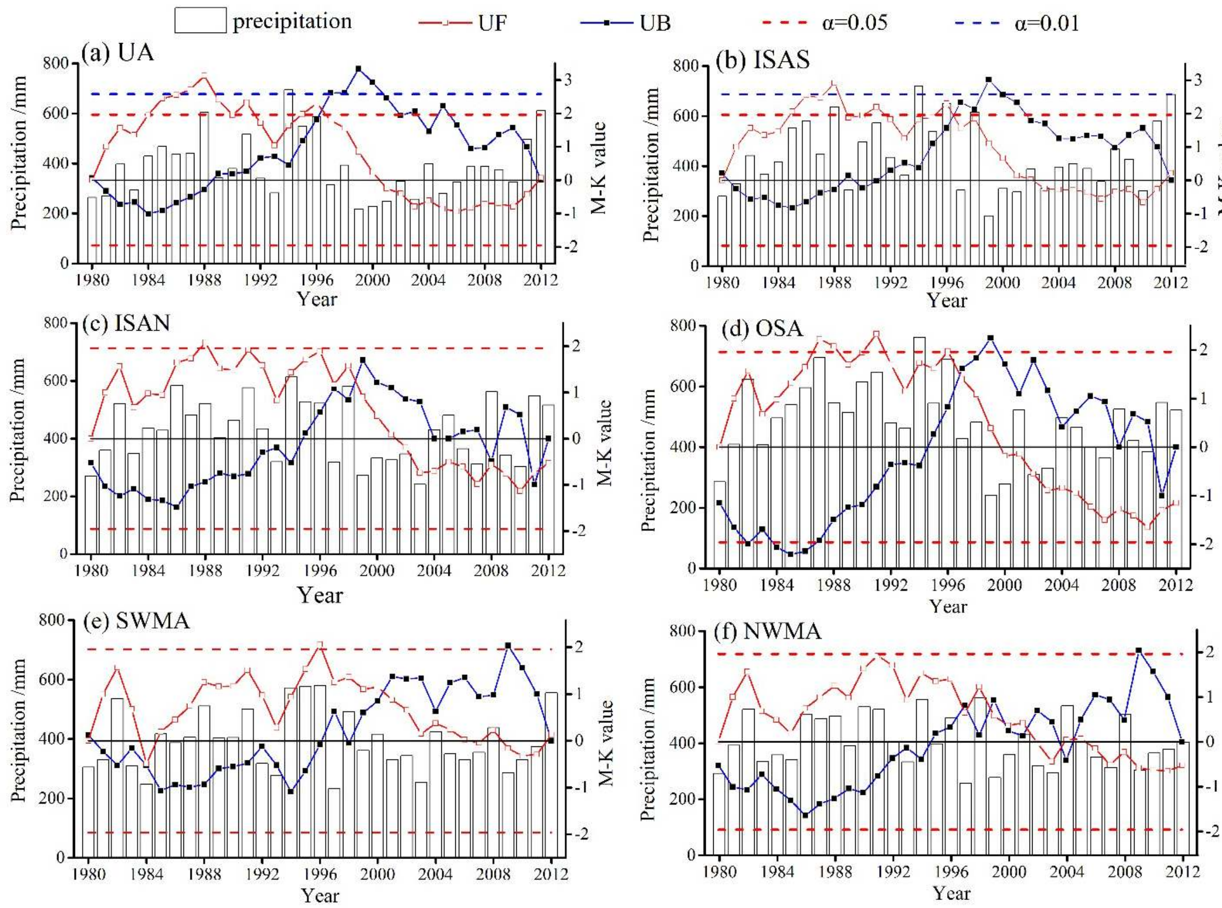

Figure 8. Time series and Mann-Kendall's testing statistics values of the precipitation amount in warm season for different parts of the Beijing area from 1980-2012.

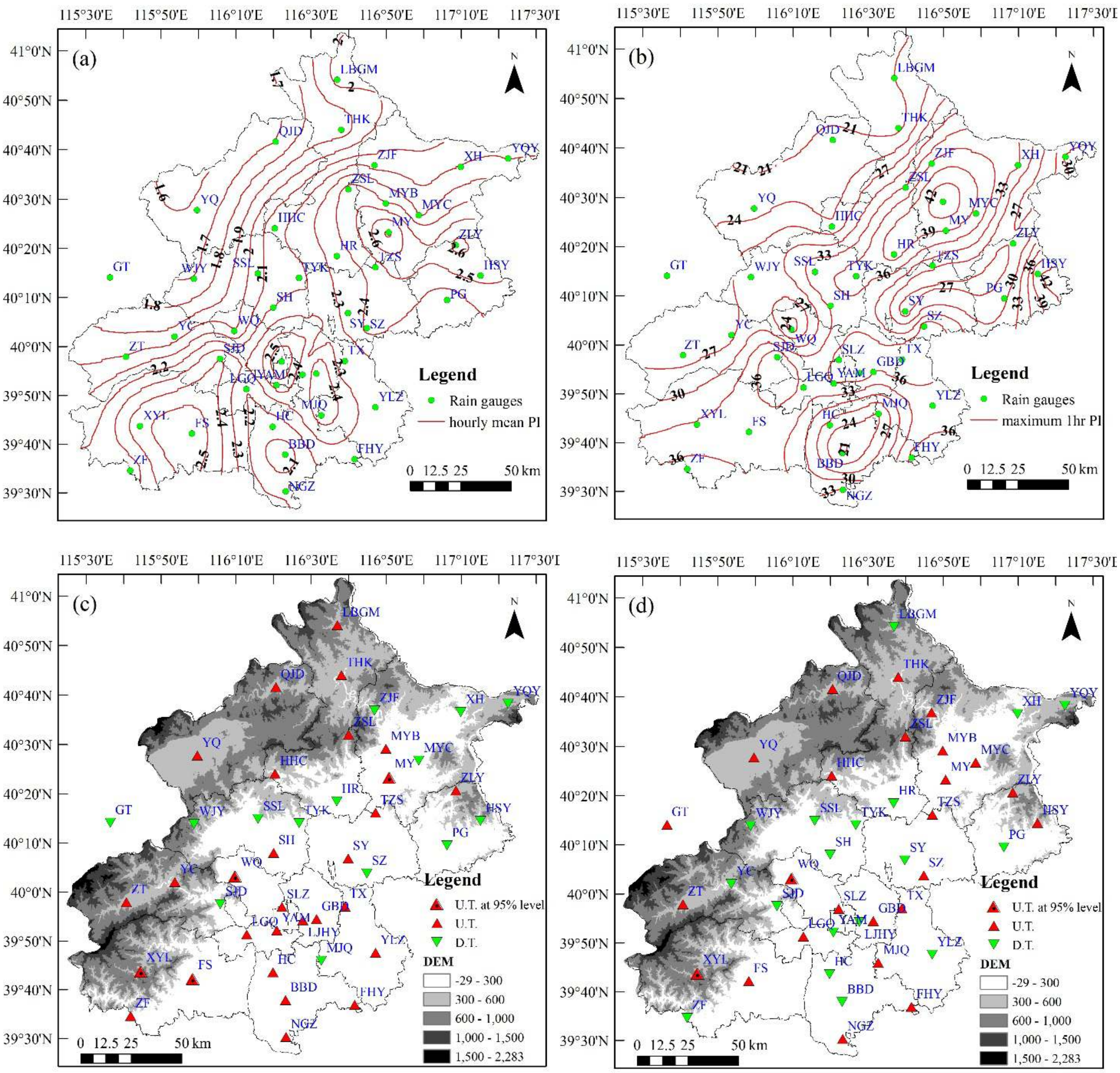

Figure 9. Spatial variation (a and b) and M-K trends (c and d) of precipitation intensity during 1980-2012. Left panel (a and c) represents the hourly mean precipitation intensity, and right panel (b, d) is the maximum 1hr precipitation intensity. PI means precipitation intensity.

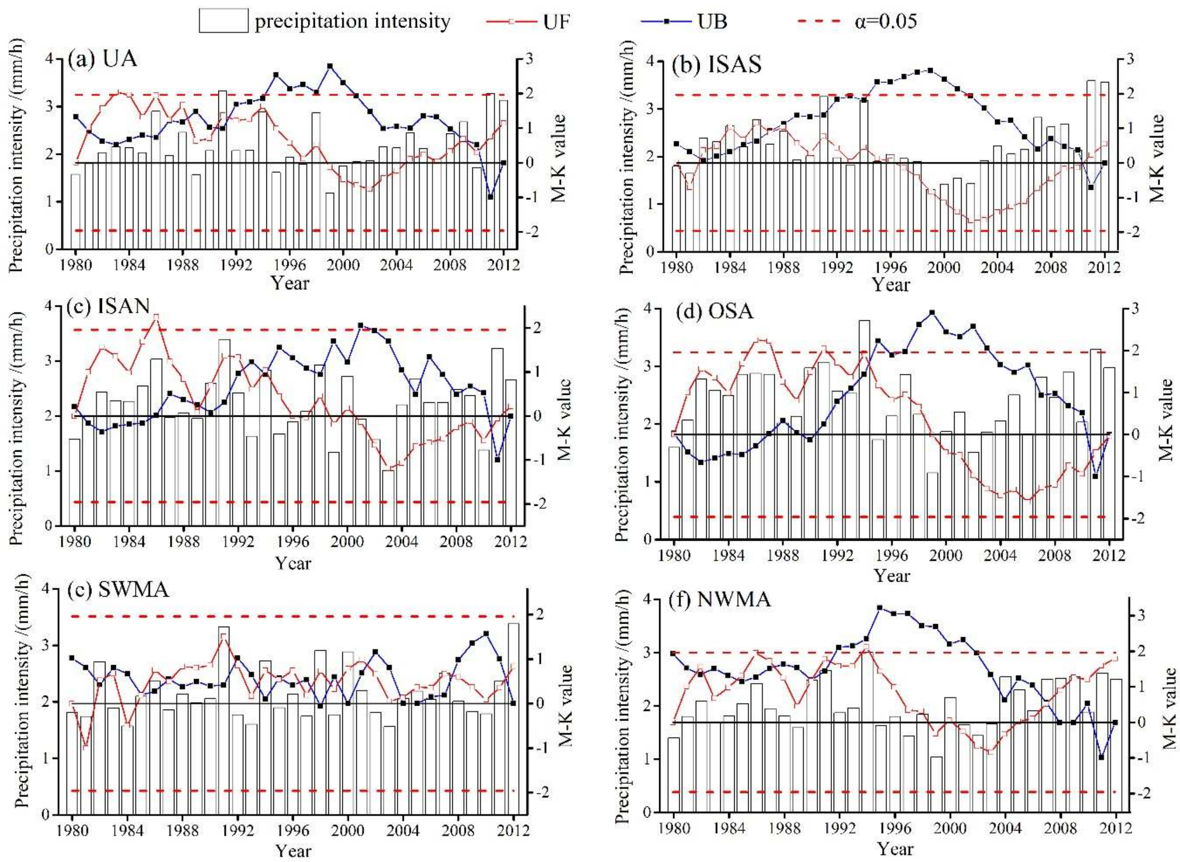

Figure 10. Time series and Mann-Kendall results of mean hourly precipitation intensity in the warm season for the six areas in the Beijing area during the past three decades

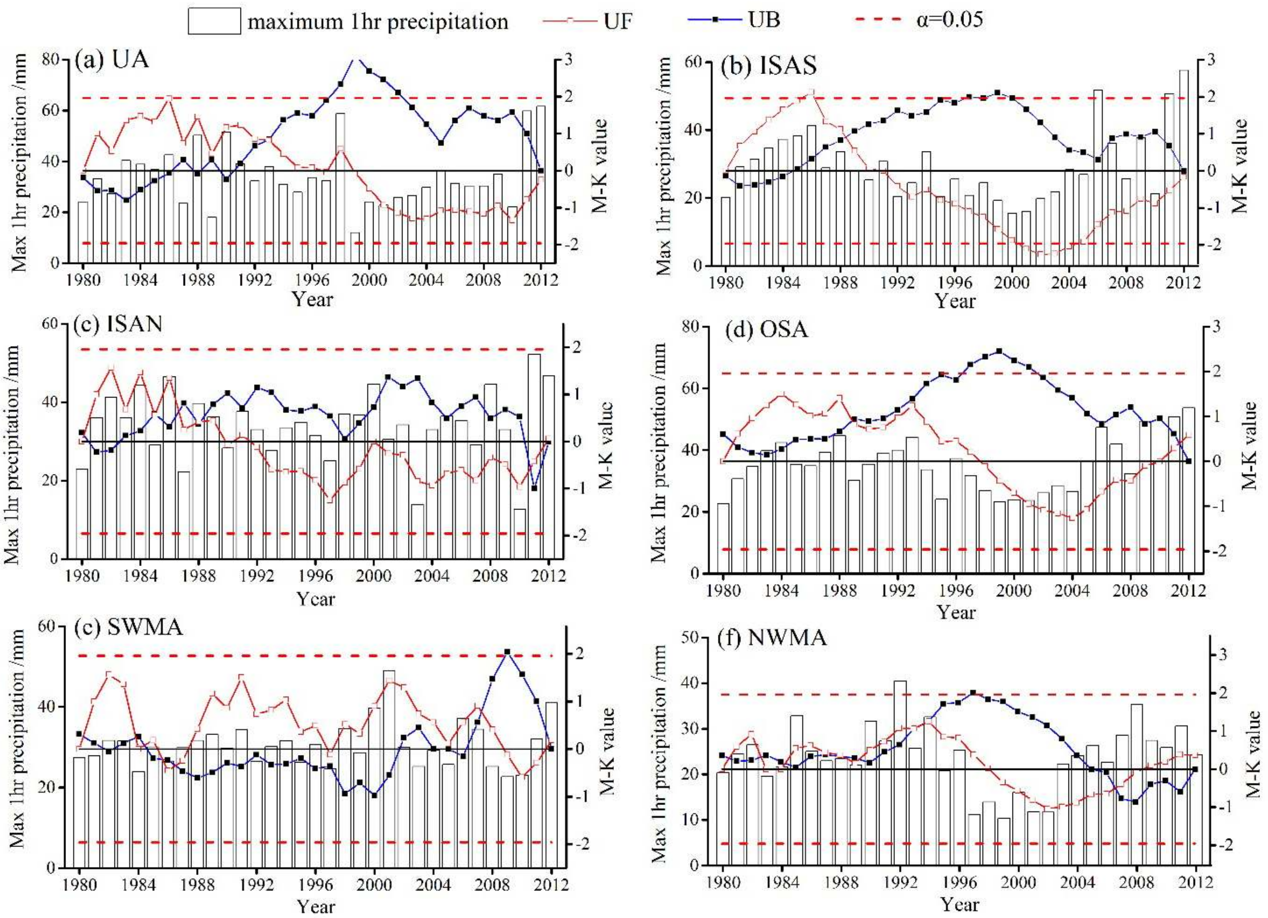

Figure 11. Time series and Mann-Kendall results of maximum 1-hour precipitation intensity in the warm season for the six areas in the Beijing area during the past three decades

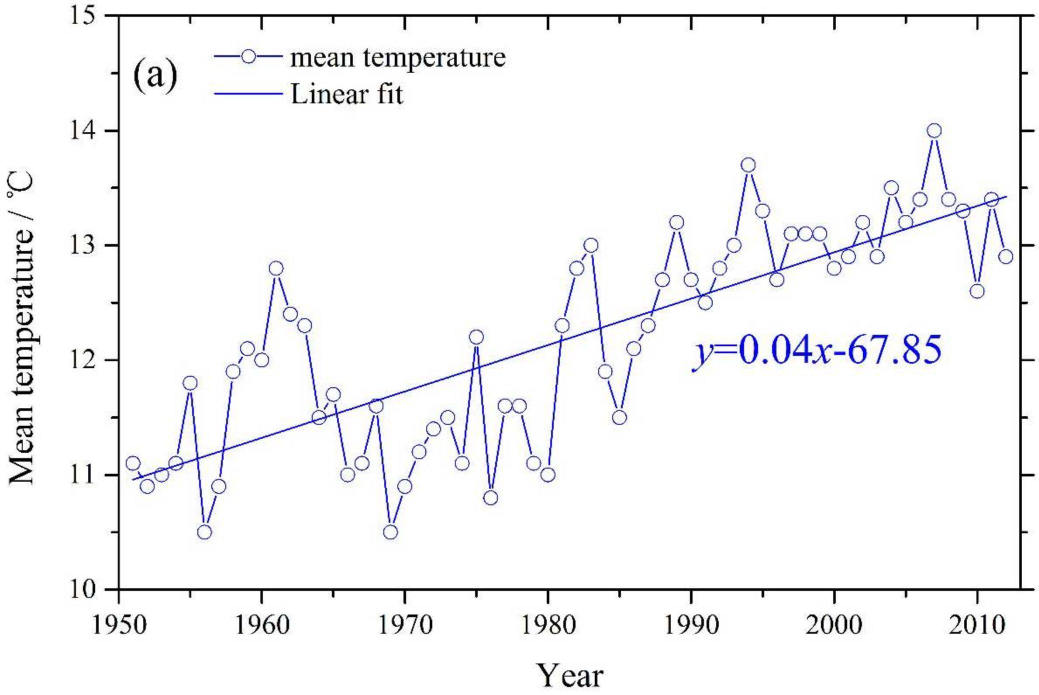

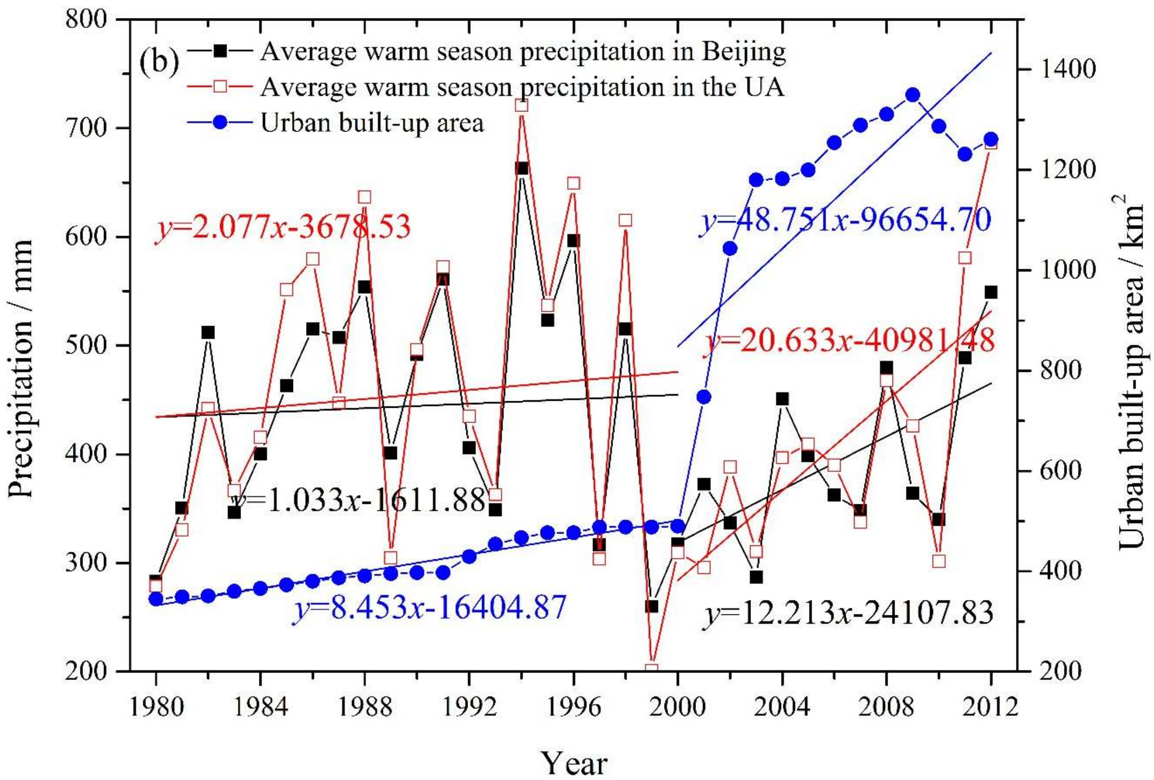

Figure 12. (a) Mean temperature for Beijing Guanxiangtai weather station during 1951-2012, and (b) the warm season precipitation and the urban built-up areas in Beijing during 1980-2012. The meaning of the lines with symbols is illustrated in the lower-left of each plot, and the lines without symbols are their corresponding linear tendency change (see linear-fitted equations).

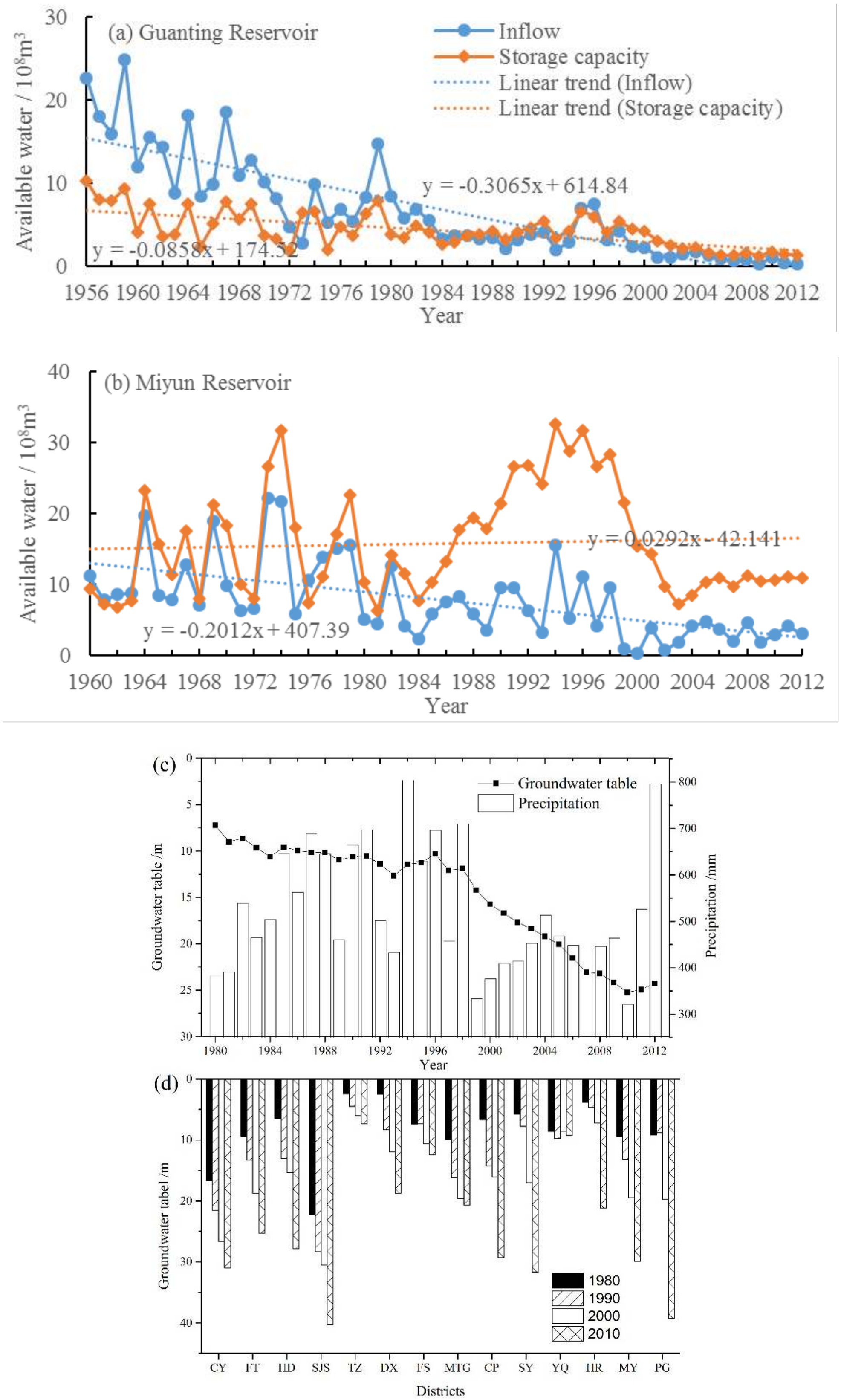

Figure 13. Variation of surface water availability in the Beijing area: variation of inflow and storage capacity for (a) the Guanting and (b) Miyun reservoirs, and variation of the groundwater table (c) in the plain areas of Beijing and (d) in the districts. CY-Chaoyang, FT-Fengtai, HD-Haidian, SJS-Shijingshan, TZ-Tongzhou, DX-Daxing, FS-Fangshan, MTG-Mengtougou, CP-Changping, SY-Shunyi, YQ-Yanqing, HR-Huairou, MY-Miyun, PG-Pinggu

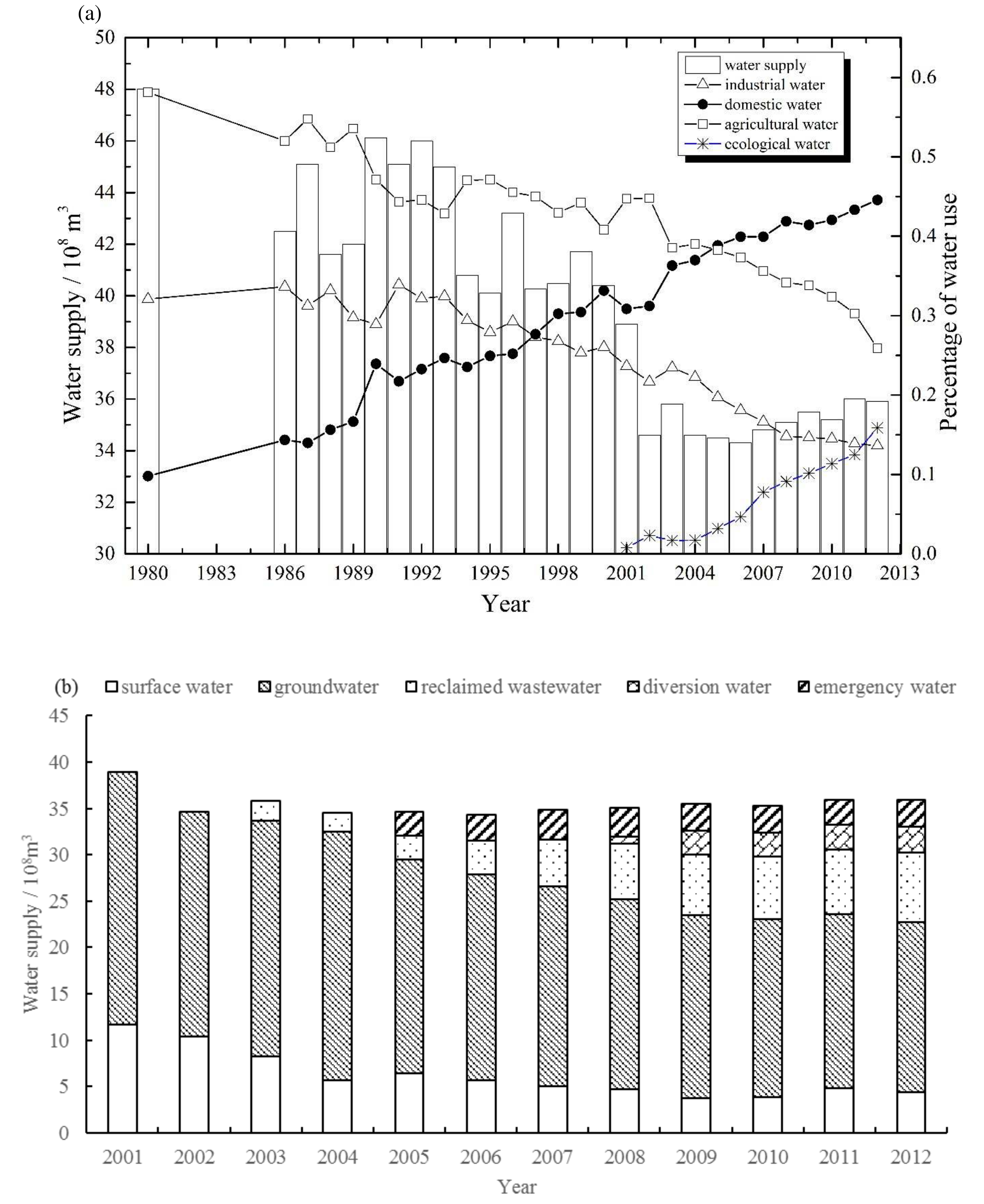

Figure 14. (a) Changes of water-use structure from 1980-2012 and (b) changes of water-use structure during 2001-2012.

Table 1 Information for all the stations and six regions in the Beijing area

Region	Station Name	Longitude/E	Latitude/N	Elevation / m
UA	Songlinzha (SLZ)	116°21'	39°57'	47
	Youanmen (YAM)	116°21'	39°52'	42
	Lejiahuayuan (LJHY)	116°27'	39°54'	37
	Gaobeidian (GBD)	116°31'	39°54'	34
	Wenquan (WQ)	116°10'	40°03'	54
	Lugouqiao (LGQ)	116°13'	39°52'	65
	Tongxian (TX)	116°39'	39°56'	23
ISAN	Shunyi (SY)	116°38'	40°07'	39
	Suzhuang (SZ)	116°45'	40°04'	33
	Shisanling reservoir (SSL)	116°16'	40°15'	84
	Shahe (SH)	116°16'	40°07'	39
	Taoyukou reservoir (TYK)	116°26'	40°14'	76
OSA	Huangsongyu reservoir (HSY)	117°15'	40°14'	198
	Pinggu (PG)	117°07'	40°08'	32
	Zhenluoying (ZLY)	117°08'	40°20'	276
	Miyunbai reservior (MYB)	116°50'	40°28'	98
	Xiahui (XH)	117°10'	40°37'	198
	Yaoqiaoyu reservoir (YQY)	117°23'	40°38'	427
	Miyunchao reservoir (MYC)	116°59'	40°27'	173
	Miyun (MY)	116°51'	40°22'	75
	Huairou reservoir (HR)	116°37'	40°18'	49
	Tangzhishan (TZS)	116°48'	40°16'	61

Region	Station Name	Longi
ISAS	Majuqiao (MJQ)	116
	Yulinzhuang (YLZ)	116
	Fengheying (FHY)	116
	Huangcun (HC)	116
	Banbidian (BBD)	116
	Fangshan (FS)	116
	Nangezhuang (NGZ)	116
NWMA	Qianjiadian (QJD)	116
	Yanqing (YQ)	115
	Labagoumen (LBGM)	116
	Tanghekou (THK)	116
	Zhangjiafen (ZJF)	116
	Huanghuacheng (HHC)	116
	Zaoshulin (ZSL)	116
SWMA	Zhaitang reservoir (ZT)	115
	Yanchi (YC)	115
	Sanjiadian (SJD)	116
	Guanting reservoir (GT)	115
	Wangjiayuan reservoir (WJY)	115
	Zhangfang (ZF)	115
	Xiayunlin (XYL)	115